

CRWMS/M&O

Calculation Cover Sheet*Complete only applicable items.*1. QA: L
Page: 1

Of: 25

2. Calculation Title HLW Canister and Can-in-Canister Drop Calculation			
3. Document Identifier (including Revision Number) BBAA00000-01717-0210-00023 REV 00			4. Total Pages 25
5. Total Attachments 4		6. Attachment Numbers - Number of pages in each I-3, II-7, III-7, and IV-2	
	Print Name	Signature	Date
7. Originator	Hongyan Marr	<i>Hongyan Marr</i>	9/7/99
8. Checker	Sreten Mastilovic	<i>Sreten Mastilovic</i>	9/15/99
9. Lead	Scott M. Bennett	<i>Scott M. Bennett</i>	09/15/99
10. Remarks			
Revision History			
11. Revision No.	12. Description of Revision		
00	Initial Issue <p style="text-align: center;">The obliterated information does not impact the technical meaning or content of the record.</p> <p style="text-align: center;"><i>Hm 9/7/99</i></p>		

CONTENTS

	Page
1. PURPOSE	3
2. METHOD	3
3. ASSUMPTIONS	3
4. USE OF COMPUTER SOFTWARE AND MODELS	5
4.1 SOFTWARE APPROVED FOR QA WORK	5
4.2 SOFTWARE ROUTINES	5
4.3 MODELS	5
5. CALCULATION	6
5.1 MATERIAL PROPERTIES	6
5.2 DESCRIPTION OF FINITE ELEMENT REPRESENTATIONS	7
5.2.1 Canister Vertical Drop (standard glass canister).....	7
5.2.2 Canister Corner Drop (standard glass canister)	9
5.2.3 Can-in-Canister Vertical Drop (glass canister containing plutonium cans)	10
5.3 EFFECT OF GLASS PROPERTIES ON THE CALCULATION.....	11
6. RESULTS	13
6.1 CANISTER VERTICAL DROP (standard glass canister).....	13
6.2 CANISTER CORNER DROP (standard glass canister)	16
6.3 CAN-IN-CANISTER VERTICAL DROP	19
6.4 EFFECT OF GLASS PROPERTIES ON THE CALCULATION.....	20
6.5 ANSYS FILES SUMMARY	21
7. REFERENCES	23
8. ATTACHMENTS	25

1. PURPOSE

The purpose of this calculation is to evaluate the structural response of the standard high-level waste (HLW) canister and the HLW canister containing the cans of immobilized plutonium ("can-in-canister" throughout this document) to the drop event during the handling operation. The objective of the calculation is to provide the structure parameter information to support the canister design and the waste handling facility design.

2. METHOD

Finite element solution is performed using the commercially available ANSYS Version (V) 5.4 finite element code. Two-dimensional (2-D) axisymmetric and three-dimensional (3-D) finite element representations for the standard HLW canister and the can-in-canister are developed and analyzed using the dynamic solver.

3. ASSUMPTIONS

- 3.1 For the can-in-canister representations, the HLW canister and its internal components (except for the plutonium-ceramic cans) including HLW glass and magazine rack are assumed to have solid connections at the adjacent surfaces. The basis for this assumption is that the design concept of the magazine rack is to pre-install the rack into the canister before pouring the glass into the canister. Therefore, the magazine rack components are assumed to have a solid contact with the glass. This assumption is used in Section 5.2.
- 3.2 The target surface is conservatively assumed to be essentially unyielding by using a large elastic modulus for the target surface compared to the canister. The basis for this assumption is that a bounding set of results is required in terms of stresses and displacements and it is known that the use of an unyielding surface ensures slightly higher stresses and displacements in the canister. Furthermore, the mass density and Poisson's ratio for unyielding target material are assumed based on the corresponding properties of concrete to meet the ANSYS V5.4 code requirements. The basis for this assumption is that concrete is most likely the target material; in addition to that these properties have negligible influence on the canister results. This assumption is used in Section 5.1.
- 3.3 Some of the temperature-dependent material properties were not available for the canister materials. Therefore, properties at room temperature (20 °C) were assumed for all materials. The basis for this assumption is that the impact of using room temperature material properties is anticipated to be small, because the mechanical properties of subject materials do not significantly change at the temperatures the canister experiences during the handling and lifting operations. This assumption is used in Section 5.1.

- 3.4 The coefficient of dynamic friction values of steel on steel contact are used on the contacting surfaces between the bottom of the canister and the target. The basis for this assumption is that although the target surface will most likely be concrete, there is no significant relative displacement between the waste package and the target surface along the plane perpendicular to the direction of impact. Thus, friction coefficients do not have a significant effect on the results. This assumption is used in Section 5.1.
- 3.5 For the can-in-canister representation, the plutonium-ceramic cans are assumed to move freely in the vertical direction inside the magazine. Further, no friction is assumed between the magazine and the cans. The basis for this assumption is that it amounts to the most conservative event by implying that during the handling operations the cans have broken away from the thin attachment to the glass. This assumption is used in Section 5.2.
- 3.6 For the can-in-canister representation, only the magazine support base plate and funnel are represented in detail. The rack radial supports, scalloped plates, and tie rods are ignored for the finite element representations (see sketches in Attachment I). The basis for this assumption is that the neglected components are not critical to the drop impact, and the simplification allows ANSYS representation to use fewer elements and to reduce code execution time. This assumption is used in Section 5.2.
- 3.7 For both standard HLW canister and can-in-canister representations, the extreme upper portion of the canister, including the neck and head, is not represented. The basis for this assumption is that they are not the critical part of the structure during the drop impact. The equivalent mass of the canister is adjusted by changing the length of the representation based on the total mass given. This assumption is used in Section 5.2.
- 3.8 Some of the rate-dependent material properties were not available for the materials used. Therefore, the material properties obtained under the static loading conditions were assumed for all materials. In general, this is a notably conservative assumption; nonetheless, in this case, the impact of using the static material properties is anticipated to be small. The basis for this assumption is that mechanical properties of subject materials do not significantly change at the peak strain rates, which occur during this event. This assumption is used in Section 5.1.

4. USE OF COMPUTER SOFTWARE AND MODELS

4.1 SOFTWARE APPROVED FOR QA WORK

The finite element computer code used for this calculation is ANSYS V5.4, which is identified by the Computer System Configuration Item (CSCI) identifier 30040 V5.4. ANSYS V5.4 is a commercially available finite element code and is appropriate for the structural analysis of the HLW canister as performed in this calculation. Calculations using the ANSYS V5.4 software were executed on a Hewlett-Packard 9000 Series (Computer Processing Unit Name: "Bloom" and Civilian Radioactive Waste Management System - Management and Operating Contractor (CRWMS-M&O) Tag Number: 700887). The software qualification of ANSYS, including problems of the type analyzed in this report, is summarized in the Software Qualification Report for ANSYS Version 5.4 (Ref. 7.3), Reference 7.14, Reference 7.15, and Reference 7.16. The ANSYS evaluations performed here are fully within the range of the validation performed for the ANSYS V5.4. Access to, and use of, the code for this calculation was granted by Software Configuration Management in accordance with the appropriate procedures.

4.2 SOFTWARE ROUTINES

None used.

4.3 MODELS

None used.

Title: HLW Canister and Can-in-Canister Drop Calculation

Document Identifier: BBAA00000-01717-0210-00023 REV 00

Page 6 of 25

5. CALCULATION

A number of data used in this calculation are based on the existing information from the current canister designs and the literature available for the material properties. Therefore, all data, excluding data considered as established facts (e.g., codes and standards, engineering handbooks), shall be treated as existing data. Use of any data from this calculation for input into documents supporting procurement, fabrication, or construction is required to be identified and tracked as TBV (to be verified) in accordance with appropriate procedures.

The number of digits in the values cited herein may be the result of a calculation or may reflect the input from another source; consequently, the number of digits should not be interpreted as an indication of accuracy.

5.1 MATERIAL PROPERTIES

Temperature-dependent and rate-dependent material properties were not available for most of the materials used in this calculation; therefore, room temperature material properties obtained under the static loading conditions were used for all materials in the calculations (Assumptions 3.3 and 3.8).

304L stainless steel (canister shell and magazine rack):

Density = 8000 kg/m³ (Ref. 7.10, p. 34)

Poisson's ratio = 0.29 (Ref. 7.10, Figure 15) (at 20 °C)

Modulus of elasticity = 195 GPa (28.3 * 10⁶ psi) (Ref. 7.8, Table TM-1) (at 20 °C)

Yield strength = 172 MPa (25 ksi) (Ref. 7.8, Table Y-1) (at 20 °C)

Tensile strength = 483 MPa (70 ksi) (Ref. 7.8, Table U) (at 20 °C)

% elongation = 40 (Ref. 7.12, Table 2) (at 20 °C)

HLW glass:

Density = 2850 kg/m³ (Ref. 7.6, Table 6.4)

Poisson's ratio = 0.2 (Ref. 7.11, p. 189) (at 20 °C)

Modulus of elasticity = 62.7 GPa (9.1 * 10⁶ psi) (Ref. 7.11, p. 189) (at 20 °C)

Ceramic (immobilized plutonium waste):

Density = 5500 kg/m³ (Ref. 7.5, p. 9)

Unyielding target:

Density = 2300 kg/m³ (Assumption 3.2)

Poisson's ratio = 0.17 (Assumption 3.2)

Modulus of elasticity = 1 * 10¹³ GPa or 1 * 10¹⁵ GPa (Assumption 3.2)

Coefficient of kinetic friction = 0.4 (steel on steel, Assumption 3.4) (Ref. 7.2, Table D/1)

The results of these impact simulations are required to include elastic and plastic deformations for the materials. When the materials are driven into the plastic range, the slope of the stress-strain curve continuously changes. Thus, a simplification for this curve is needed to incorporate plasticity into the finite element representation. A standard approximation is commonly used in engineering by assuming a straight line that connects the yield point to the ultimate tensile strength point of the material (see Fig. 5.1-1).

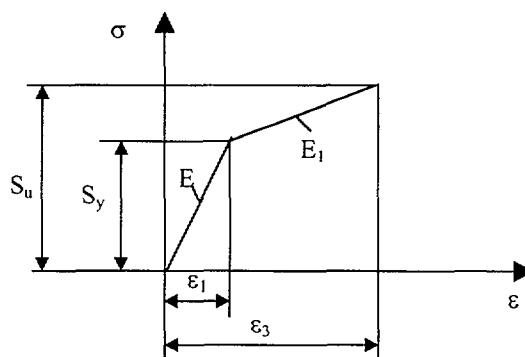


Figure 5.1-1. Stress-Strain Curve

where:

S_y = Yield strength

S_u = Ultimate tensile strength

ϵ_1, ϵ_3 = Strain magnitudes (corresponding to yield strength and elongation, respectively)

E = Elastic modulus (slope of the stress-strain line in the elastic region)

E_1 = Tangent modulus (slope of the stress-strain line in the plastic region)

The slope, E_1 , is determined by:
$$E_1 = \frac{S_u - S_y}{\epsilon_3 - \epsilon_1}$$

where: $\epsilon_1 = S_y / E$

For stainless steel 304L:

$$E_1 = (0.483 - 0.172) / (0.40 - (0.172 / 195)) = 0.779 \text{ GPa}$$

5.2 DESCRIPTION OF FINITE ELEMENT REPRESENTATIONS

5.2.1 Canister Vertical Drop (standard glass canister)

To calculate the structural response of the HLW glass canister to a vertical drop, a 2-D axisymmetric representation is developed to take advantage of the symmetric geometry of the canister. The 2-D representation includes the canister shell containing the glass waste form. The very top portion of the canister, including neck and head, are not represented since they are not the critical parts of the

Title: HLW Canister and Can-in-Canister Drop Calculation**Document Identifier:** BBAA00000-01717-0210-00023 REV 00Page 8 of 25

structure during the drop (free fall) impact. The equivalent mass of the upper volume is adjusted to the lower portion of the volume (Assumption 3.7). The canister is assumed to drop onto an unyielding target surface, characterized by a very large modulus of elasticity (Assumption 3.2). Four drop heights are evaluated: 7 m, 8 m, 9 m, and 11.58 m. To reduce the computer execution time, the simulation is started from a position where the canister is about to contact the unyielding surface. The corresponding canister velocities just before the contact are calculated based on the initial drop heights at velocity of zero. The following describes the detailed information of the calculation.

- 1) The total canister mass (2580 kg) used in the calculation is obtained by adjusting the canister length to match the mass of can-in-canister heavy configuration (2600 kg) indicated in Table 2 of Ref. 7.7. This mass is most likely to bound all the glass canister mass with or without plutonium disposition.
- 2) Canister velocity at contact position is determined based on the following:

$$V = g \cdot t = g \cdot \sqrt{\frac{2 \cdot H}{g}} \quad (\text{Equation 5.2.1-1})$$

where: H = drop height (m)

g = gravitational acceleration = 9.81 m/s²

t = time (s)

thus, for 7-m drop, H1=7 m, V1=11.713 m/s

8-m drop, H2=8 m, V2=12.527 m/s

9-m drop, H3=9 m, V3=13.293 m/s

11.58-m (38-feet) drop, H4=11.58 m, V4=15.078 m/s

- 3) Dynamic amplification factor calculation at the time of impact - In some situations, the dynamic problems can be approximated under static load conditions with application of a dynamic amplification factor. To estimate the impact of the canister to the vertical drop, a dynamic amplification factor calculation is performed at a drop height of 7 m. The way of incorporating the dynamic amplification factor for impact is to determine, if the load is statically applied, what factor is needed to multiply to the same load to result in the same magnitude of stress as the impact. Thus, the same 2-D axisymmetric representation is used under static condition to determine the dynamic amplification factor. In this representation, the mass of the canister is scaled with factors of 1000, 1500, 1800, and 1650. By comparing the maximum stresses of the static and dynamic calculations, the dynamic amplification factor for the 7-m drop can be determined. This factor is later used in Section 5.2.3.

The ANSYS representations of the vertical drop are displayed on pages II-1 and II-2 of Attachment II.

5.2.2 Canister Corner Drop (standard glass canister)

To simulate another drop event during the handling, a corner canister drop is evaluated. The orientation of the corner drop, which aligns the canister center of gravity with the canister bottom corner along the same vertical line, provides the maximum linear momentum for the canister to convert potential energy to deformation energy. Figure 5.2-1 shows the initial drop orientation for the canister at vertical and corner drops.

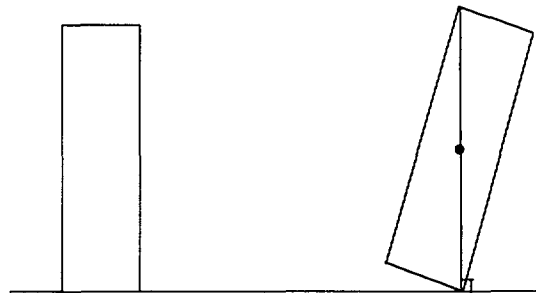


Figure 5.2-1. Orientation of Vertical and Corner Drops

To calculate the structural response of the HLW glass canister to the corner drop, a half-symmetry 3-D representation of the canister is constructed. The 3-D representation includes the canister shell and the glass waste form. The very top portion of the canister, including neck and head, is not represented since they are not the critical parts of the structure during the drop impact. The equivalent mass of the upper volume is adjusted to the lower portion of the volume (Assumption 3.7). The canister is assumed to drop onto an unyielding target surface with a very large modulus of elasticity specified for the target material (Assumption 3.2). Several drop heights including 2 m, 4 m, 7 m, and 9.14 m are evaluated. To reduce the execution time, the ANSYS simulation is started from a position where the canister is about to contact the unyielding surface. The corresponding canister velocities just before the contact are calculated based on the initial drop heights at velocity of zero. The following describes the detailed information of the calculation.

- 1) The total canister mass (2531 kg) used in the calculation is obtained by adjusting the canister length to match the mass of can-in-canister heavy configuration (2600 kg) indicated in Table 2 of Ref. 7.7. This mass is most likely to bound all the glass canister mass with or without plutonium disposition.
- 2) Canister velocity at contact position is determined based on the following:

$$V = g \cdot t = g \cdot \sqrt{\frac{2 \cdot H}{g}} \quad (\text{Equation 5.2.2-1})$$

where: H = drop height (m)

g = gravitational acceleration = 9.81 m/s²

t = time (s)

thus, for 2-m drop, H1=2 m, V1=6.269 m/s
4-m drop, H2=4 m, V2=8.858 m/s
7-m drop, H3=7 m, V3=11.713 m/s
9.14-m drop, H4=9.14 m, V4=13.391 m/s

The ANSYS representations of the corner drop are displayed on pages III-1 and III-2 of Attachment III.

5.2.3 Can-in-Canister Vertical Drop (glass canister containing plutonium cans)

A 3-D finite element representation of the can-in-canister design is developed to determine the effect of the vertical drop on the canister and magazine support. The 3-D finite element representation is developed using the dimensions provided in Attachment I. Since there are 7 magazines, evenly spaced about the canister center axis, a 1/14 slice of the canister is used in the calculation. The slice captures almost the whole length of the canister except for the canister neck and head. The representation includes the magazine rack base and glass; however, it excludes the portion of the plutonium cans. The rack radial supports, scalloped plates, and tie rods are ignored (see sketches in Attachment I) to simplify the representation and reduce the execution time (Assumption 3.6).

The computer simulation of the can-in-canister dropping from a certain height takes two steps. First, the canister and the magazines are falling at the same velocity before the canister reaches the target surface. Second, once the canister contacts the target surface, the impact takes place. With the deceleration of the canister, the impact between the canister bottom and target surface, and between the magazine and the magazine support occurs. The method for calculating the structural response of the canister with additional impact on the magazine base cone is approximated by applying a constant pressure on the base funnel surface after the canister contacts the target surface. The pressure applied on the base funnel surface and the glass area is determined from the estimated dynamic amplification factor of the 7-m vertical drop of canister, as described in Section 5.2.1. The following describes the details of mass and pressure calculation.

1) Mass Calculation

Total canister mass = 2600 kg (Ref. 7.7, p. 3)

Total magazine mass = empty can mass + ceramic mass + magazine mass
= 112 lb + 640 lb + 185 lb (Ref. 7.7, Table 2)
= 937 lb
= 425 kg

Mass of canister without magazine = 2600 kg – 425 kg = 2175 kg

2) Pressure Calculation

The pressure, resulting from the dynamic impact of the magazine, is assumed to be exerted on the base funnel (A1) and the glass surface (A2) near the magazine tip (Figure 5.2-2). Since the problem is statically indeterminate, it is assumed that the forces exerted on the cone

surface and glass surface result in the same deformation in both directions at the same time. Thus the pressures on both surfaces are assumed to be the same.

Thus,

$$P = \frac{F_1}{A_1} = \frac{F_2}{A_2} \quad (\text{Equation 5.2.3-1})$$

$$\text{Also, } \frac{F_1}{\sin \theta} + F_2 = M \cdot f \cdot g \quad (\text{Equation 5.2.3-2})$$

where:

M = total mass of one magazine = $425.4/7 = 60.8$ kg

F_1 = force exerted on the cone surface

F_2 = force exerted on the glass surface

f = dynamic amplification factor = 1650 (determined from Section 5.2.1, see results in Section 6.1)

g = gravitational acceleration = 9.81 m/s²

$\theta = 28.76^\circ$ (Attachment I, p. I-2)

A_1 = base funnel surface area (Table 6.6-1, File # 55) = 0.0118 m²

A_2 = glass surface area (Table 6.6-1, File # 55) = $5.07 \cdot 10^{-4}$ m²

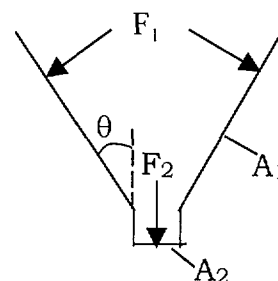


Figure 5.2-2. Base Funnel

Solving Equations 5.2.3-1 and 5.2.3-2, the pressure exerted on the cone surface and glass surface can be found to be $P = 3.92 \cdot 10^7$ N/m².

In addition, to evaluate the stress increase from the impact of an additional magazine, a comparison between the canister with and without magazine is performed. The same 3-D representation was run under the same condition, but no pressure was added to the support cone.

The ANSYS representations of the can-in-canister drop are displayed on pages IV-1 and IV-2 of Attachment IV.

5.3 EFFECT OF GLASS PROPERTIES ON THE CALCULATION

The HLW glass canister contains borosilicate glass, which is considered brittle material. The stress-strain behavior of brittle material under compression is dependent on the geometry of the material component and loading conditions. Since there is little information available for glass properties and also since the stress on the canister shell instead of the stress on the glass is of interest, an elastic-perfectly-brittle model is generally used in the calculation. In actuality, under the compressive load, the brittle material will experience non-linear stress-strain curve due to the gradual development of the microcracking within the material after the critical stress (Ref. 7.4, p. 42). Therefore, to evaluate the effect of the glass properties on the calculation, bilinear elastic-plastic stress-strain curves are used to evaluate the sensitivity of the results. The compressive strength of the glass is conservatively

used to evaluate the sensitivity of the results. The compressive strength of the glass is conservatively assumed to be 500 MPa (Ref. 7.9, p. 18). The slope in hardening region is assumed to be half of the elastic slope. Other variations, e.g., critical stress of 200 MPa, and slope of one-twentieth of the elastic slope are also evaluated. Figure 5.3-1 shows the four glass stress-strain curves used in the calculation.

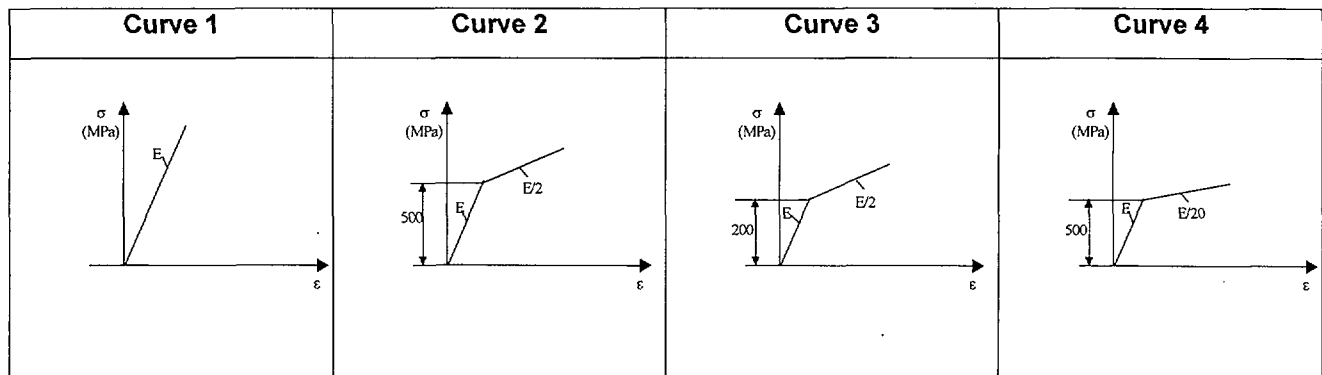


Figure 5.3-1. Stress-Strain Curves for the Glass

6. RESULTS

The results obtained from this calculation are based on the existing information from the current canister package designs and the literature available for material properties. Although some data are obtained from accepted sources such as American Society of Mechanical Engineers (ASME) Boiler and Pressure Vessel Code, or American Society for Testing and Materials (ASTM) Specifications, all results provided in this document are to be verified. Use of any data or results from this calculation for input into documents supporting procurement, fabrication, or construction is required to be identified and tracked as TBV in accordance with appropriate procedures.

6.1 CANISTER VERTICAL DROP (standard glass canister)

The structural response of the canister (standard glass) to vertical drops is reported using both strain and stress intensity values at the times when they reach the maximum. For all drop heights analyzed (7 m, 8 m, 9 m, and 11.58 m), the maximum strain and stress from the drop impact on the canister shell occur at the bottom surface portion of the canister, which contacts the target surface first.

Since the canister shell experiences the highest stress and strain at the location where contact occurs, and the tension in the direction along the target surface seems to be critical for the shell material to develop the rupture openings, the strain values in the direction parallel to the target surface are listed in Tables 6.1-1 through 6.1-4 for the drop heights of 7 m, 8 m, 9 m, and 11.58 m, respectively. Page II-3 of Attachment II displays the locations of the nodes used in the tables. Pages II-4 through II-7 show the strain contours on the canister shell.

For all the drop heights analyzed, the maximum strain values through the shell thickness along the target surface direction do not appear to be exceeding the elongation of the material (304L) of 40%.

Table 6.1-1. Strain Through Canister Shell for 7-m Vertical Drop (Table 6.6-1, File # 5)
(at the time when the strain on canister shell reaches
the maximum [Table 6.6-1, File #4, line 4170])

Location 1		Location 2		Location 3		Location 4		Location 5	
Node #	ϵ_x	Node #	ϵ_x	Node #	ϵ_x	Node #	ϵ_x	Node #	ϵ_x
146	0.10	93	0.10	104	0.07	103	0.11	102	0.18
153	0.09	94	0.21	129	0.19	125	0.08	121	0.09
154	0.05	95	0.31	130	0.25	126	0.03	122	0.01
155	0.05	96	0.35	131	0.25	127	-0.01	123	-0.02
156	0.06	97	0.35	132	0.23	128	-0.03	124	-0.05
134	0.07	85	0.31	92	0.19	91	-0.94e-3	90	-0.03

Table 6.1-2. Strain Through Canister Shell for 8-m Vertical Drop (Table 6.6-1, File # 10)
(at the time when the strain on canister shell reaches
the maximum [Table 6.6-1, File #9, line 3594])

Location 1		Location 2		Location 3		Location 4		Location 5	
Node #	ϵ_x	Node #	ϵ_x	Node #	ϵ_x	Node #	ϵ_x	Node #	ϵ_x
146	0.11	93	0.10	104	0.07	103	0.11	102	0.18
153	0.10	94	0.22	129	0.19	125	0.09	121	0.10
154	0.07	95	0.32	130	0.25	126	0.03	122	0.02
155	0.07	96	0.37	131	0.26	127	-0.59e-2	123	-0.02
156	0.07	97	0.37	132	0.23	128	-0.02	124	-0.05
134	0.07	85	0.34	92	0.19	91	0.51e-2	90	-0.03

Table 6.1-3. Strain Through Canister Shell for 9-m Vertical Drop (Table 6.6-1, File # 15)
(at the time when the strain on canister shell reaches
the maximum [Table 6.6-1, File #14, line 4098])

Location 1		Location 2		Location 3		Location 4		Location 5	
Node #	ϵ_x	Node #	ϵ_x	Node #	ϵ_x	Node #	ϵ_x	Node #	ϵ_x
146	0.11	93	0.11	104	0.07	103	0.11	102	0.20
153	0.11	94	0.23	129	0.19	125	0.09	121	0.11
154	0.08	95	0.33	130	0.26	126	0.04	122	0.02
155	0.08	96	0.39	131	0.27	127	0.11e-2	123	-0.02
156	0.08	97	0.39	132	0.24	128	-0.02	124	-0.05
134	0.08	85	0.37	92	0.20	91	0.01	90	-0.03

Table 6.1-4. Strain Through Canister Shell for 11.58-m Vertical Drop (Table 6.6-1, File # 20)
(at the time when the strain on canister shell reaches
the maximum [Table 6.6-1, File #19, line 3846])

Location 1		Location 2		Location 3		Location 4		Location 5	
Node #	ϵ_x	Node #	ϵ_x	Node #	ϵ_x	Node #	ϵ_x	Node #	ϵ_x
146	0.11	93	0.11	104	0.07	103	0.11	102	0.22
153	0.13	94	0.24	129	0.20	125	0.11	121	0.13
154	0.12	95	0.35	130	0.29	126	0.06	122	0.04
155	0.12	96	0.42	131	0.29	127	0.01	123	-0.01
156	0.10	97	0.45	132	0.25	128	-0.02	124	-0.05
134	0.10	85	0.43	92	0.21	91	0.02	90	-0.03

The stress intensity of the canister shell is reported at the time when it reaches the maximum. For all drop heights analyzed (7 m, 8 m, 9 m, and 11.58 m), the maximum stress from the drop impact on the canister shell occurs at the bottom surface portion of the canister, which contacts the target surface first. Tables 6.1-5 through 6.1-8 list the stress intensity as nodal results for 7-m, 8-m, 9-m, and 11.58-m vertical drops. It should be noted that since the bilinear stress-strain curve is used within the stress range up to an ultimate tensile strength of 483 MPa, any stresses above that value are linearly extrapolated by ANSYS. Thus, the characteristics of the ruptured material can not be simulated, and overestimated stress may be reported in one part of those high-deformation regions while on the other hand, due to the shielding effect, the underestimated stresses may be reported in the neighboring nodes.

Table 6.1-5. Stress Intensity Through Canister Shell for 7-m Vertical Drop (Table 6.6-1, File # 3)
(at the time when shell stress reaches the maximum [Table 6.6-1, File #2, line 3417])

Location 1		Location 2		Location 3		Location 4		Location 5	
Node #	σ, int^* (MPa)	Node #	σ, int (MPa)	Node #	σ, int (MPa)	Node #	σ, int (MPa)	Node #	σ, int (MPa)
146	421	93	270	104	391	103	556	102	465
153	416	94	430	129	401	125	437	121	433
154	386	95	532	130	411	126	368	122	385
155	400	96	580	131	320	127	334	123	367
156	388	97	577	132	343	128	338	124	322
134	144	85	542	92	404	91	255	90	288

* int – stress intensities

Table 6.1-6. Stress Intensity Through Canister Shell for 8-m Vertical Drop (Table 6.6-1, File #8)
(at the time when shell stress reaches the maximum [Table 6.6-1, File #7, line 3021])

Location 1		Location 2		Location 3		Location 4		Location 5	
Node #	σ, int (MPa)	Node #	σ, int (MPa)	Node #	σ, int (MPa)	Node #	σ, int (MPa)	Node #	σ, int (MPa)
146	412	93	270	104	408	103	542	102	473
153	413	94	430	129	460	125	458	121	424
154	382	95	544	130	460	126	361	122	340
155	409	96	599	131	412	127	319	123	308
156	411	97	603	132	424	128	310	124	280
134	254	85	570	92	413	91	230	90	268

Table 6.1-7. Stress Intensity Through Canister Shell for 9-m Vertical Drop (Table 6.6-1, File #13)
(at the time when shell stress reaches the maximum [Table 6.6-1, File #12, line 3120])

Location 1		Location 2		Location 3		Location 4		Location 5	
Node #	σ, int (MPa)	Node #	σ, int (MPa)	Node #	σ, int (MPa)	Node #	σ, int (MPa)	Node #	σ, int (MPa)
146	441	93	269	104	423	103	584	102	494
153	458	94	446	129	471	125	487	121	449
154	427	95	556	130	486	126	396	122	374
155	440	96	617	131	478	127	362	123	379
156	423	97	627	132	436	128	344	124	351
134	280	85	602	92	416	91	228	90	301

Table 6.1-8. Stress Intensity Through Canister Shell for 11.58-m Vertical Drop (Table 6.6-1, File #18)
(at the time when shell stress reaches the maximum [Table 6.6-1, File #17, line 3186])

Location 1		Location 2		Location 3		Location 4		Location 5	
Node #	σ, int (MPa)	Node #	σ, int (MPa)	Node #	σ, int (MPa)	Node #	σ, int (MPa)	Node #	σ, int (MPa)
146	451	93	270	104	452	103	629	102	538
153	489	94	448	129	504	125	533	121	481
154	472	95	574	130	524	126	427	122	405
155	475	96	651	131	521	127	368	123	395

156	452	97	684	132	474	128	326	124	360
134	307	85	675	92	431	91	208	90	292

The dynamic amplification factors for 7-m drop are determined by comparing the maximum stress from the static simulation with factors of 1000, 1500, 1800, and 1650, with the dynamic simulation. The results listed in Table 6.1-9 indicate that the static simulation with the dynamic amplification factor of 1650 results in approximately the same maximum stress as does the 7-m vertical drop simulation.

Table 6.1-9. Canister Shell Stress Intensity at Different Dynamic Amplification Factors

Dynamic Amplification Factor	Maximum Stress Intensity in the Canister Shell (MPa)
7-m Dynamic Drop Case	580 (Table 6.6-1, File #3, line 327)
1000	420 (Table 6.6-1, File #22, line 304)
1500	538 (Table 6.6-1, File #24, line 304)
1650	575 (Table 6.6-1, File #28, line 304)
1800	612 (Table 6.6-1, File #26, line 304)

6.2 CANISTER CORNER DROP (standard glass canister)

The structural response of the canister (standard glass) to corner drops is reported using both strain and stress intensity values at the times when they reach the maximum. For all drop heights analyzed (2 m, 4 m, 7 m, and 9.14 m), the maximum strain and stress from the drop impact on the canister shell occur at the localized corner area on the bottom of the canister.

Since the localized canister shell corner experiences the highest stress and strain at the location where contact occurs, and the tension in the direction along the target surface seems to be critical for shell material to develop the rupture openings, the strain values in the direction parallel to the target surface are listed in Tables 6.2-1 through 6.2-4 for the drop heights of 2 m, 4 m, 7 m, and 9.14 m, respectively. Page III-3 of Attachment III displays the locations of the nodes used in the tables. Pages III-4 through III-7 show the strain contours on the canister shell.

For all the drop heights analyzed, although very high strain is developed on the outer portion of the shell, the maximum strain values along the target surface direction, through the shell thickness, do not exceed the elongation of the material (304L) of 40%.

Title: HLW Canister and Can-in-Canister Drop Calculation

Document Identifier: BBAA00000-01717-0210-00023 REV 00

Page 17 of 25

Table 6.2-1. Strain Through Canister Shell for 2-m Corner Drop (Table 6.6-1, File #34)
(at the time when shell strain reaches the maximum [Table 6.6-1, File #33, line 2837])

Location 1		Location 2		Location 3		Location 4		Location 5	
Node #	ϵ_x	Node #	ϵ_x	Node #	ϵ_x	Node #	ϵ_x	Node #	ϵ_x
94	0.25	55	-0.07	64	0.19	63	-0.06	62	0.26
97	0.14	56	0.11	81	0.38	77	0.05	73	0.17
98	0.53e-2	57	0.28	82	0.59	78	0.13	74	0.06
99	-0.06	58	0.32	83	0.71	79	0.10	75	-0.02
100	-0.12	59	0.30	84	0.68	80	0.08	76	-0.05
86	-0.11	49	0.29	54	0.62	53	0.08	52	-0.04

Table 6.2-2. Strain Through Canister Shell for 4-m Corner Drop (Table 6.6-1, File #39)
(at the time when shell strain reaches the maximum [Table 6.6-1, File #38, line 3567])

Location 1		Location 2		Location 3		Location 4		Location 5	
Node #	ϵ_x	Node #	ϵ_x	Node #	ϵ_x	Node #	ϵ_x	Node #	ϵ_x
94	0.18	55	-0.34	64	0.23	63	-0.19	62	0.20
97	0.07	56	-0.84e-2	81	0.45	77	-0.01	73	0.14
98	-0.02	57	0.32	82	0.70	78	0.16	74	0.07
99	-0.05	58	0.38	83	0.89	79	0.13	75	-0.02
100	-0.11	59	0.34	84	0.85	80	0.10	76	-0.05
86	-0.09	49	0.33	54	0.74	53	0.10	52	-0.05

Table 6.2-3. Strain Through Canister Shell for 7-m Corner Drop (Table 6.6-1, File #44)
(at the time when shell strain reaches the maximum [Table 6.6-1, File #43, line 3855])

Location 1		Location 2		Location 3		Location 4		Location 5	
Node #	ϵ_x	Node #	ϵ_x	Node #	ϵ_x	Node #	ϵ_x	Node #	ϵ_x
94	-0.02	55	-0.65	64	0.26	63	-0.37	62	0.08
97	-0.08	56	-0.15	81	0.51	77	-0.10	73	0.09
98	-0.06	57	0.37	82	0.76	78	0.18	74	0.07
99	-0.04	58	0.49	83	1.01	79	0.15	75	-0.02
100	-0.10	59	0.40	84	0.98	80	0.13	76	-0.05
86	-0.07	49	0.38	54	0.81	53	0.15	52	-0.04

Table 6.2-4. Strain Through Canister Shell for 9.14-m Corner Drop (Table 6.6-1, File #50)
(at the time when shell strain reaches the maximum [Table 6.6-1, File #49, line 2005])

Location 1		Location 2		Location 3		Location 4		Location 5	
Node #	ϵ_x	Node #	ϵ_x	Node #	ϵ_x	Node #	ϵ_x	Node #	ϵ_x
94	-0.13	55	-0.82	64	0.25	63	-0.50	62	-0.03
97	-0.15	56	-0.23	81	0.54	77	-0.15	73	0.03
98	-0.06	57	0.37	82	0.79	78	0.21	74	0.07
99	-0.03	58	0.52	83	1.07	79	0.18	75	-0.02
100	-0.09	59	0.41	84	1.07	80	0.16	76	-0.06
86	-0.06	49	0.36	54	0.89	53	0.20	52	-0.04

The structural response of the canister (standard glass) to corner drop is also reported using stress intensity values at the time when the stress intensity in the canister shell reaches the maximum. For all drop heights analyzed (2 m, 4 m, 7 m, and 9.14 m), the maximum stress from the drop impact on the canister shell occurs at a localized corner area on the bottom of the canister. Tables 6.2-5 through 6.2-8 list the maximum stress intensities through the shell thickness for different drop heights. It should be noted that since the bilinear stress-strain curve is used within the stress range up to ultimate tensile strength of 483 MPa, any stresses above that value are linearly extrapolated by ANSYS. Thus, the characteristics of the ruptured material can not be simulated, and overestimated stress may be reported in one part of those high-deformation region while on the other hand, due to the shielding effect, the underestimated stresses may be reported in the neighboring nodes.

Table 6.2-5. Stress Intensity Through Canister Shell for 2-m Corner Drop (Table 6.6-1, File #32)
(at the time when shell stress reaches the maximum [Table 6.6-1, File #31, line 2493])

Location 1		Location 2		Location 3		Location 4		Location 5	
Node #	σ , int (MPa)	Node #	σ , int (MPa)	Node #	σ , int (MPa)	Node #	σ , int (MPa)	Node #	σ , int (MPa)
94	287	55	725	64	552	63	584	62	175
97	249	56	759	81	659	77	702	73	153
98	380	57	453	82	801	78	389	74	272
99	416	58	259	83	955	79	243	75	287
100	318	59	223	84	975	80	324	76	103
86	151	49	293	54	950	53	305	52	165

Table 6.2-6. Stress Intensity Through Canister Shell for 4-m Corner Drop (Table 6.6-1, File #37)
(at the time when shell stress reaches the maximum [Table 6.6-1, File #36, line 2996])

Location 1		Location 2		Location 3		Location 4		Location 5	
Node #	σ , int (MPa)	Node #	σ , int (MPa)	Node #	σ , int (MPa)	Node #	σ , int (MPa)	Node #	σ , int (MPa)
94	376	55	1186	64	541	63	824	62	399
97	283	56	1018	81	696	77	803	73	165
98	291	57	622	82	803	78	443	74	263
99	451	58	329	83	1026	79	235	75	285
100	387	59	241	84	1079	80	205	76	167
86	300	49	407	54	1073	53	188	52	226

Table 6.2-7. Stress Intensity Through Canister Shell for 7-m Corner Drop (Table 6.6-1, File #42)
(at the time when shell stress reaches the maximum [Table 6.6-1, File #41, line 3260])

Location 1		Location 2		Location 3		Location 4		Location 5	
Node #	σ , int (MPa)	Node #	σ , int (MPa)	Node #	σ , int (MPa)	Node #	σ , int (MPa)	Node #	σ , int (MPa)
94	757	55	1556	64	457	63	1033	62	619
97	574	56	1166	81	641	77	999	73	293
98	384	57	574	82	752	78	532	74	361
99	591	58	352	83	1114	79	331	75	284
100	484	59	320	84	938	80	152	76	164
86	522	49	296	54	1093	53	348	52	201

Table 6.2-8. Stress Intensity Through Canister Shell for 9.14-m Corner Drop (Table 6.6-1, File #48)
(at the time when shell stress reaches the maximum [Table 6.6-1, File #47, line 1551])

Location 1		Location 2		Location 3		Location 4		Location 5	
Node #	σ , int (MPa)	Node #	σ , int (MPa)	Node #	σ , int (MPa)	Node #	σ , int (MPa)	Node #	σ , int (Mpa)
94	1560	55	1731	64	385	63	1476	62	1533
97	1378	56	1325	81	494	77	1190	73	1130
98	1000	57	916	82	672	78	719	74	698
99	651	58	636	83	1277	79	299	75	640
100	446	59	393	84	957	80	196	76	466
86	261	49	499	54	1238	53	346	52	319

6.3 CAN-IN-CANISTER VERTICAL DROP

The structural response of the can-in-canister to the 7-m vertical drop is reported using both strain and stress intensity values at the times when they reach their maximums. Since a constant pressure resulting from the maximum dynamic amplification factor was applied on the rack base funnel, the strain and stress results from this approximation are slightly conservative.

The maximum strain and stress from the drop impact on the canister shell occur at the bottom surface area of the canister, which first contacts the target surface. The strain magnitude along the target surface direction in the canister shell does not exceed the elongation of the material (40%) through the shell thickness at the area of contact.

In addition, the vertical drop without magazine (no pressure applied on the support cone) is performed to compare the stresses and strains. Table 6.3-1 lists the maximum strains along the target surface direction for the two cases. Table 6.3-2 lists the maximum stress intensity resulting from the two calculations. The maximum strain and stress intensity increases at the contact area due to the additional magazine impact are not significant.

Table 6.3-1. Maximum Strain Through Canister Shell for Can-in-Canister Vertical Drop

	Maximum Strain on the Inner Surface of the Shell	Maximum Strain Inside the Shell	Maximum Strain on the Outer Surface of the Shell
Without magazine	0.11 (Table 6.6-1, File #54, line 299)	0.26 (Table 6.6-1, File #53, line 2960)	0.23 (Table 6.6-1, File #54, line 399)
With magazine	0.12 (Table 6.6-1, File #59, line 300)	0.27 (Table 6.6-1, File #58, line 3741)	0.23 (Table 6.6-1, File #59, line 400)

Table 6.3-2. Maximum Stress Intensity Through Canister Shell for Can-in-Canister Vertical Drop

	Maximum Stress Intensity on the Inner Surface of the Shell (MPa)	Maximum Stress Intensity Inside the Shell (MPa)	Maximum Stress Intensity on the Outer Surface of the Shell (MPa)	Maximum Stress Intensity in the Support Funnel (MPa)
Without magazine	349 (Table 6.6-1, File #52, line 10727)	515 (Table 6.6-1, File #52, line 2740)	463 (Table 6.6-1, File #52, line 10946)	N/A*
With magazine	348 (Table 6.6-1, File #57, line 10707)	519 (Table 6.6-1, File #57, line 3224)	473 (Table 6.6-1, File #57, line 10926)	210 (Table 6.6-1, File #57, line 6950)

* N/A – not applicable

6.4 EFFECT OF GLASS PROPERTIES ON THE CALCULATION

The effect of glass properties on the calculation is reported using stress values obtained from the finite element solution of the problem. The maximum stress intensities in the glass and the canister shell are compared for different glass stress-strain curves (see Figure 5.3-1). The stress results are listed in Table 6.4-1.

The results show that for the assumed glass properties, the stresses in the glass are highly dependent on the stress-strain curve that the glass will experience under compressive load. The assumed linear stress-strain curve (Figure 5.3-1, curve 1) produces the highest stresses in the glass, as expected. The stress change in the canister shell due to the change of glass properties is not so pronounced. Assuming glass properties as being elastic produces the most conservative calculation results. In summary, since the canister shell is of interest for this calculation, using curve 1 of Figure 5.3-1 throughout the calculation gives reasonable and slightly conservative stress results in the canister.

Table 6.4-1. Strain and Stress Comparison for Varying Glass Properties

Curve No.	Maximum Stress Intensity in the Canister Shell (MPa)	Maximum Stress Intensity in the Glass (MPa)
1	515 (File #52, line 2740, Table 6.6-1)	1764 (File #52, line 5029, Table 6.6-1)
2	506 (File #61, line 2377, Table 6.6-1)	1212 (File #61, line 4897, Table 6.6-1)
3	500 (File #63, line 2495, Table 6.6-1)	1213 (File #63, line 4454, Table 6.6-1)
4	480 (File #65, line 2683, Table 6.6-1)	790 (File #65, line 5079, Table 6.6-1)

6.5 ANSYS FILES SUMMARY

The ANSYS files listed in Table 6.5-1 include the output files, which record the input commands and solution process. The additional post-processing files used to extract the results for each case analyzed are also listed. All files are stored on a compact disk (CD) (Ref. 7.13).

Table 6.5-1. ANSYS File Summary

#	File Name	Description	Size (kb)	Date	Time
Vertical Drop					
1	/axi2_fin/axi2_fin.out	7-m vertical drop	353	6/24/99	1:26 PM
2	/axi2_fin/maxshl.out		197	6/24/99	1:26 PM
3	/axi2_fin/sint1.out		28	6/24/99	1:26 PM
4	/axi2_fin/eptot.out		235	7/21/99	4:29 PM
5	/axi2_fin/eptot1.out		29	7/21/99	4:29 PM
6	/axi3_fin/axi3_fin.out	8-m vertical drop	338	6/24/99	1:23 PM
7	/axi3_fin/maxshl.out		180	6/24/99	1:25 PM
8	/axi3_fin/sint1.out		28	6/24/99	1:23 PM
9	/axi3_fin/eptot.out		216	7/21/99	4:30 PM
10	/axi3_fin/eptot1.out		29	7/21/99	4:30 PM
11	/axi5_fin/axi5_fin.out	9-m vertical drop	362	6/24/99	1:30 PM
12	/axi5_fin/maxshl.out		197	6/24/99	1:30 PM
13	/axi5_fin/sint1.out		28	6/24/99	1:30 PM
14	/axi5_fin/eptot.out		235	7/21/99	4:31 PM
15	/axi5_fin/eptot1.out		29	7/21/99	4:31 PM
16	/axi4_fin/axi4_fin.out	11.58-m vertical drop	342	6/24/99	1:31 PM
17	/axi4_fin/maxshl.out		187	6/24/99	1:31 PM
18	/axi4_fin/sint1.out		28	6/24/99	1:31 PM
19	/axi4_fin/eptot.out		223	7/21/99	4:30 PM
20	/axi4_fin/eptot1.out		29	7/21/99	4:30 PM
Dynamic Amplification Factor					
21	/saxi2_f1/saxi2_f1.out	f =1000	147	6/24/99	1:32 PM
22	/saxi2_f1/sint.out		16	6/24/99	1:32 PM
23	/saxi2_f2/saxi2_f2.out	f =1500	148	6/24/99	1:33 PM
24	/saxi2_f2/sint.out		16	6/24/99	1:33 PM

Waste Package Operations

Calculation

Title: HLW Canister and Can-in-Canister Drop Calculation

Document Identifier: BBAA00000-01717-0210-00023 REV 00

Page 22 of 25

25	/saxi2_f3/saxi2_f3.out	f =1800	147	6/24/99	1:35 PM
26	/saxi2_f3/sint.out		16	6/24/99	1:35 PM
27	/saxi2_f4/saxi2_f4.out	f =1650	147	6/24/99	1:37 PM
28	/saxi2_f4/sint.out		16	6/24/99	1:37 PM
Corner Drop					
29	/cdrp4/cdrp4.out	2-m corner drop	567	8/2/99	11:10 AM
30	/cdrp4/rcdrp4.out		67	8/2/99	11:10 AM
31	/cdrp4/maxshl.out		134	8/2/99	11:10 AM
32	/cdrp4/sint1.out		28	8/2/99	11:10 AM
33	/cdrp4/eptot.out		159	8/2/99	11:10 AM
34	/cdrp4/eptot1.out		30	8/2/99	11:10 AM
35	/cdrp3/cdrp3.out	4-m corner drop	619	8/2/99	11:10 AM
36	/cdrp3/maxshl.out		163	8/2/99	11:10 AM
37	/cdrp3/sint1.out		28	8/2/99	11:10 AM
38	/cdrp3/eptot.out		195	8/2/99	11:10 AM
39	/cdrp3/eptot1.out		30	8/2/99	11:10 AM
40	/cdrp1/cdrp1.out	7-m corner drop	622	8/2/99	11:09 AM
41	/cdrp1/maxshl.out		179	8/2/99	11:09 AM
42	/cdrp1/sint1.out		28	8/2/99	11:09 AM
43	/cdrp1/eptot.out		214	8/2/99	11:09 AM
44	/cdrp1/eptot1.out	30	8/2/99	11:09 AM	
45	/cdrp6/cdrp6.out	9.14-m corner drop	594	8/2/99	11:10 AM
46	/cdrp6/rcdrp6.out		94	8/2/99	11:10 AM
47	/cdrp6/maxshl.out		97	8/2/99	11:10 AM
48	/cdrp6/sint1.out		28	8/2/99	11:10 AM
49	/cdrp6/eptot.out		114	8/2/99	11:10 AM
50	/cdrp6/eptot1.out		30	8/2/99	11:10 AM
Can-in-Canister Vertical Drop					
51	/tst7_66e/tst66e.out	7-m drop (without magazine) curve 1	485	6/24/99	1:46 PM
52	/tst7_66e/sint.out		532	6/24/99	1:46 PM
53	/tst7_66e/eptot.out	full-length representation	160	7/21/99	4:32 PM
54	/tst7_66e/eptot1.out		20	7/21/99	4:32 PM
55	/mag7_d1/mag7_d1.out	7-m drop (with magazine)	475	6/24/99	1:44 PM
56	/mag7_d1/rmag7_d1.out		75	6/24/99	1:44 PM
57	/mag7_d1/sint.out		532	6/24/99	1:44 PM
58	/mag7_d1/eptot.out		209	7/21/99	4:40 PM
59	/mag7_d1/eptot1.out		20	7/21/99	4:40 PM
Glass Properties					
60	/tst7_88e/tst7_88e.out	curve 2	487	6/24/99	1:45 PM
61	/tst7_88e/sint.out		509	6/24/99	1:45 PM
62	/tst7_99e/tst7_99e.out	curve 3	481	6/24/99	1:47 PM
63	/tst7_99e/sint.out		446	6/24/99	1:47 PM
64	/tst7_10e/tst7_10e.out	curve 4	464	6/24/99	1:49 PM
65	/tst7_10e/sint.out		492	6/24/99	1:49 PM

7. REFERENCES

- 7.1 Not Used.
- 7.2 Meriam, J.L. and Kraige, L.G. 1987. *Engineering Mechanics, Volume 1, Statics*. Second Edition. pp. 441, 443. New York, New York: John Wiley and Sons, Inc. TIC: 241293.
- 7.3 CRWMS M&O 1998. *Software Qualification Report for ANSYS V5.4. CSCI: 30040 V5.4. 30040-2003 REV 00*. Las Vegas, Nevada: M&O. ACC: MOL.19980609.0847.
- 7.4 MacGregor, J.G. 1997. *Reinforced Concrete: Mechanics and Design*. Third Edition. Upper Saddle River, New Jersey: Prentice Hall. TIC: 242587
- 7.5 CRWMS M&O 1999. *Can-in-Canister Concept Information and Data Report*. Interoffice Correspondence (IOC): LV.WP.AAA.06/99-108. Las Vegas, Nevada: M&O. ACC: MOL.19990625.0237.
- 7.6 Stout, R.B. and Leider, H. 1994. *Preliminary Waste Form Characteristics Report Version 1.0*. UCRL-ID-108314 Rev 1. Livermore, California: Lawrence Livermore National Laboratory. TIC: 213843.
- 7.7 Jones, R.H. 1998. *Weight of Can-in-Canister Assembly*. Interoffice Memorandum: NMP-PLS-980153. Aiken, South Carolina: Westinghouse Savannah River Company. TIC: 243808.
- 7.8 American Society of Mechanical Engineers (ASME) 1995. *1995 ASME Boiler and Pressure Vessel Code*. Section II. New York, New York: ASME. TIC: 241170.
- 7.9 Mencik, J. 1992. *Strength and Fracture of Glass and Ceramics*. New York, New York: Elsevier Science Publishing Company, Inc. TIC: 245277.
- 7.10 American Society for Metals (ASM) 1980. *Metals Handbook Ninth Edition, Volume 3, Properties and Selection: Stainless Steels, Tool Materials and Special-Purpose Metals*. Metals Park, Ohio: ASM. TIC: 209801.
- 7.11 Lewis, C.F., ed. 1990. *Materials Engineering, Material Selector 1991*. pp. 105, 188, and 189. Cleveland, Ohio: Penton Publishing. TIC: 239718.
- 7.12 American Society for Testing and Materials (ASTM) 1997. *Standard Specification for Heat-Resisting Chromium and Chromium-Nickel Stainless Steel Plate, Sheet, and Strip for Pressure Vessels*. ASTM Designation: A 240/A 240M-97a. West Conshohocken, Pennsylvania: ASTM. TIC: 239431.

Title: HLW Canister and Can-in-Canister Drop Calculation

Document Identifier: BBAA00000-01717-0210-00023 REV 00

Page 24 of 25

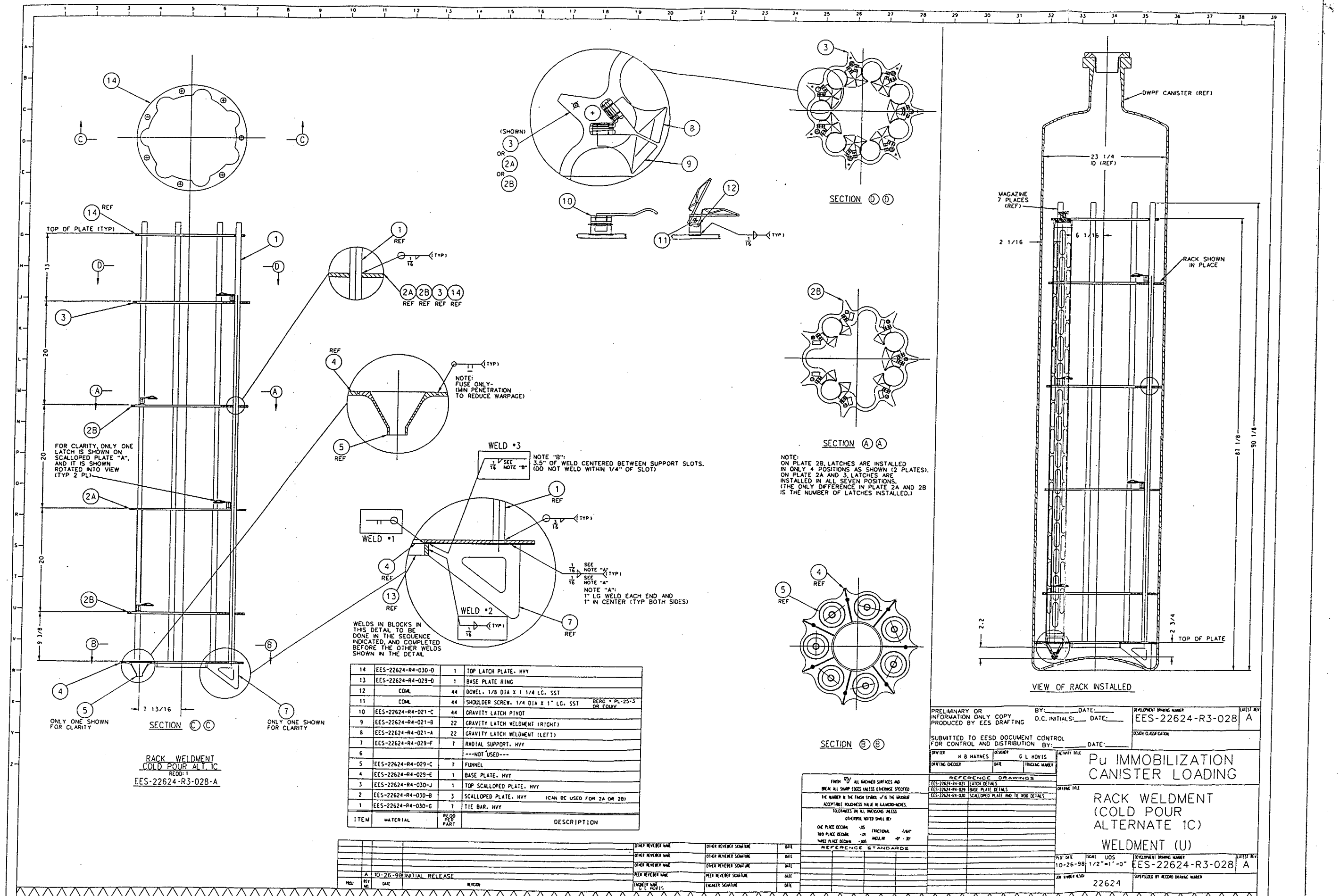
- 7.13 CRWMS M&O 1999. *Electronic Files for: HLW Canister and Can-in-Canister Drop Calculation, BBAA00000-01717-0210-00023 REV 00.* Las Vegas, Nevada: M&O. ACC: MOL.19990819.0268.
- 7.14 CRWMS M&O 1998. *Qualification of ANSYS V5.4 on the WPO HP UNIX Workstations.* IOC: LV.WP.SMB.05/98-100. Las Vegas, Nevada: M&O. ACC: MOL.19980730.0147.
- 7.15 CRWMS M&O 1998. *Qualification of ANSYS V5.4 on New WPO HP UNIX Workstation.* IOC: LV.WP.MML.11/98-220. Las Vegas, Nevada: M&O. ACC: MOL.19981217.0106.
- 7.16 CRWMS M&O 1999. *Qualification of ANSYS V5.4 on Three New WPO HP UNIX Workstations.* IOC: LV.WP.SMB.05/99-071. Las Vegas, Nevada: M&O. ACC: MOL.19990518.0322.

8. ATTACHMENTS

The attachments to this calculation are summarized in Table 8-1.

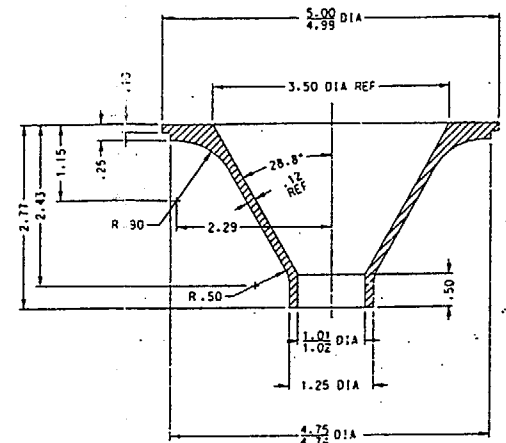
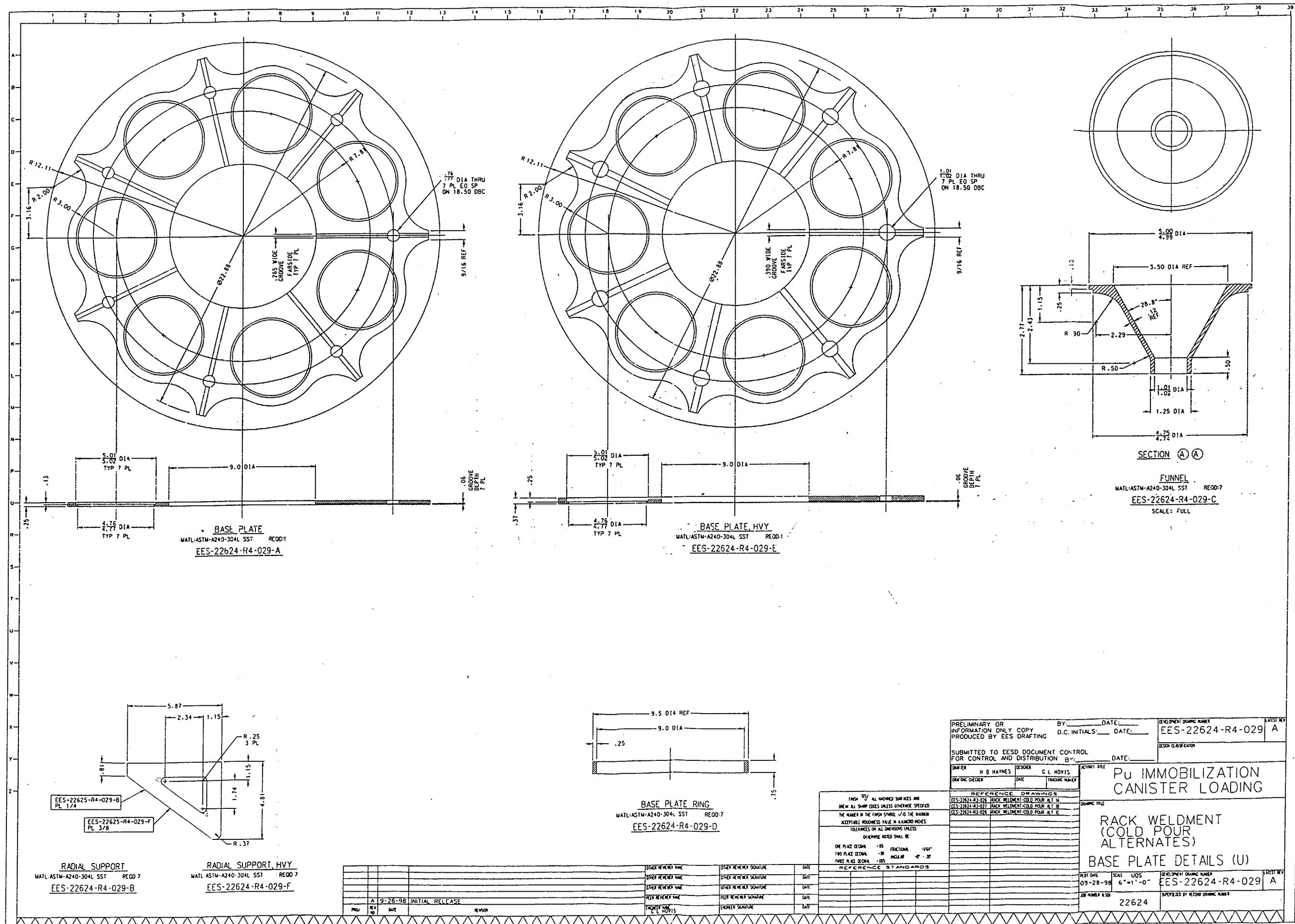
Table 8-1. Attachments Summary

Attachment Number	Description	Pages
I	Magazine Design Sketches	3
II	Vertical Drop Meshes and Stress Contours	7
III	Corner Drop Meshes and Stress Contours	7
IV	Can-in-Canister Vertical Drop Meshes	2

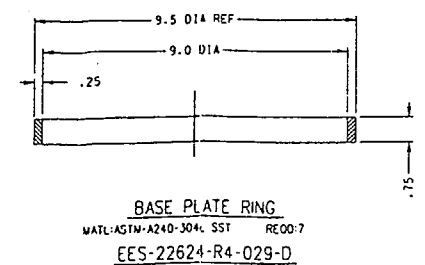
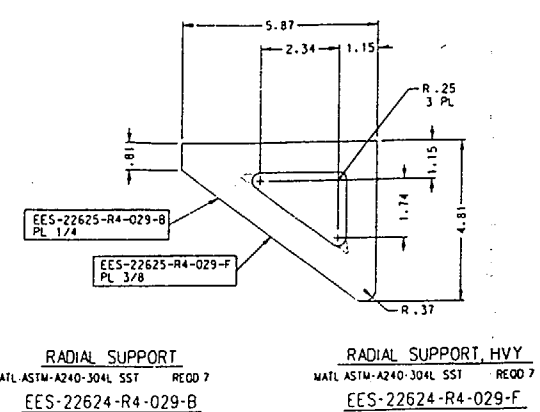


ITEM	MATERIAL	QTY PER PART	DESCRIPTION
14	EES-22624-R4-030-D	1	TOP LATCH PLATE, HVY
13	EES-22624-R4-029-D	1	BASE PLATE RING
12	CDML	44	DOWEL, 1/8 DIA X 1 1/4 LG, SST
11	CDML	44	SHOULDER SCREW, 1/4 DIA X 1" LG, SST
10	EES-22624-R4-021-C	44	GRAVITY LATCH PIVOT
9	EES-22624-R4-021-B	22	GRAVITY LATCH WELDMENT (RIGHT)
8	EES-22624-R4-021-A	22	GRAVITY LATCH WELDMENT (LEFT)
7	EES-22624-R4-029-F	7	RADIAL SUPPORT, HVY
6			---NOT USED---
5	EES-22624-R4-029-C	7	FUNNEL
4	EES-22624-R4-029-E	1	BASE PLATE, HVY
3	EES-22624-R4-030-J	1	TOP SCALLOPED PLATE, HVY
2	EES-22624-R4-030-B	3	SCALLOPED PLATE, HVY (CAN BE USED FOR 2A OR 2B)
1	EES-22624-R4-030-G	7	TIE BAR, HVY

PRELIMINARY OR INFORMATION ONLY COPY PRODUCED BY EES DRAFTING		BY: _____ DATE: _____	DEVELOPMENT DRAWING NUMBER: EES-22624-R3-028	LATEST REV: A
SUBMITTED TO EESD DOCUMENT CONTROL FOR CONTROL AND DISTRIBUTION BY: _____ DATE: _____		DESIGN CLASSIFICATION		
DRAWER: H B HAYNES	DESIGNER: G L HOVIS	ACTIVITY DATE	DRAWING TITLE	
DRAWING CHECKER	DATE	TRACING NUMBER	Pu IMMOBILIZATION CANISTER LOADING	
REFERENCE DRAWINGS		DRAWING TITLE		
EES-22624-R4-021 LATCH DETAILS		RACK WELDMENT (COLD POUR ALTERNATE 1C)		
EES-22624-R4-029 BASE PLATE DETAILS		WELDMENT (U)		
EES-22624-R4-030 SCALLOPED PLATE AND TIE ROD DETAILS		EES-22624-R3-028		
TOLERANCES UNLESS OTHERWISE SPECIFIED:		SUPERSEDED BY RECORD DRAWING NUMBER		
ONE PLACE DECIMAL: .05 FRACTIONAL: 1/64"		22624		
TWO PLACE DECIMAL: .01 FRACTIONAL: 1/32"		10-26-98		
THREE PLACE DECIMAL: .005 FRACTIONAL: 1/200"		SCALE: 1/2" = 1'-0"		
REFERENCE STANDARDS		DEVELOPMENT DRAWING NUMBER: EES-22624-R3-028		
OTHER REVISIONS		LATEST REV: A		
DATE		DATE		
DATE		DATE		
DATE		DATE		
DATE		DATE		

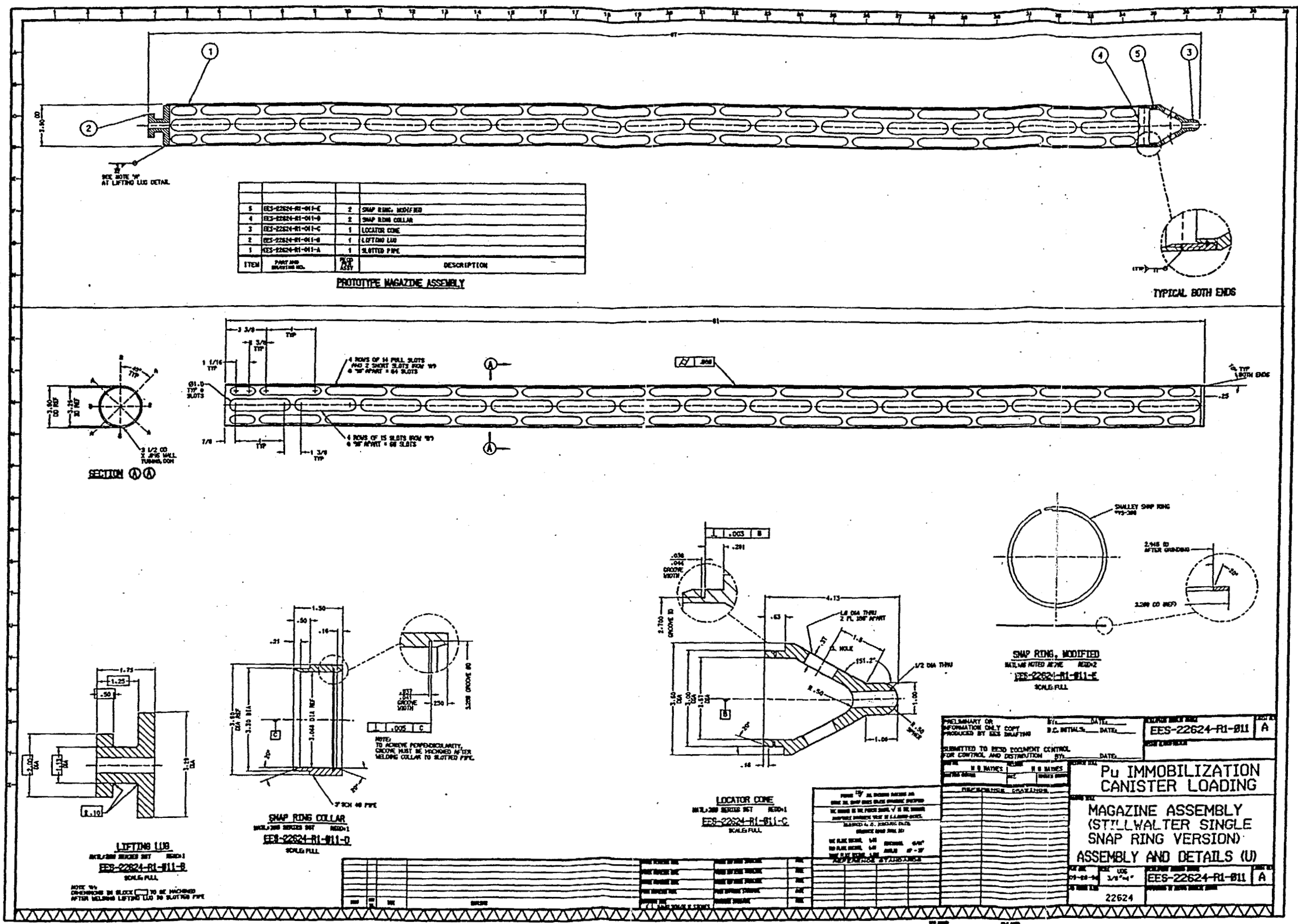


SECTION (A) (A)
 FUNNEL
 MATL:ASTM-A240-304L SST RECD:7
 EES-22624-R4-029-C
 SCALE: FULL



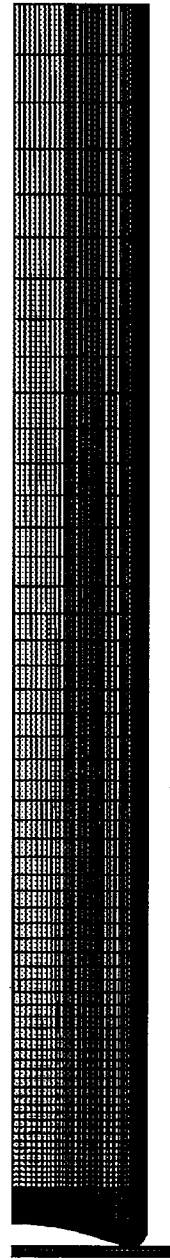
PRELIMINARY OR INFORMATION ONLY COPY PRODUCED BY EES DRAFTING		BY: _____ DATE: _____	DEVELOPMENT DRAWING NUMBER: EES-22624-R4-029	REVISION: A
SUBMITTED TO EES DOCUMENT CONTROL FOR CONTROL AND DISTRIBUTION		DATE: _____	DESIGN CLASSIFICATION	
DRAWN BY: H B HAYNES	CHECKED BY: G L HOVIS	ACTIVITY DATE	Pu IMMOBILIZATION CANISTER LOADING	
REFERENCE DRAWINGS: EES-22624-R4-029 RACK WELDMENT-COLD POUR ALT A EES-22624-R4-027 RACK WELDMENT-COLD POUR ALT B EES-22624-R4-028 RACK WELDMENT-COLD POUR ALT C		DRAWING TITLE: RACK WELDMENT (COLD POUR ALTERNATES) BASE PLATE DETAILS (U)		
FINISH: ALL WORKED SURFACES AND DRILL ALL SHARP EDGES UNLESS OTHERWISE SPECIFIED		PROJECT DATE: 09-28-98		
TOLERANCES: THE NUMBER IN THE FRACTION SHALL BE ACCEPTABLE UNLESS NOTED OTHERWISE		SCALE: UOS 6"=1'-0"		
TOLERANCES ON ALL DIMENSIONS UNLESS OTHERWISE NOTED SHALL BE: ONE PLACE DECIMAL: .10 FRACTIONAL: .004" TWO PLACE DECIMAL: .01 INCHES: .004" THREE PLACE DECIMAL: .005		DEVELOPMENT DRAWING NUMBER: EES-22624-R4-029		
REFERENCE STANDARDS		JOB NUMBER: 22624		
PROJ: _____	REV: _____	DATE: _____	REVISION: _____	DATE: _____

PROJ	REV	DATE	REVISION	DESIGNER NAME	DESIGNER SIGNATURE	DATE
A	9-26-98		INITIAL RELEASE	G L HOVIS		





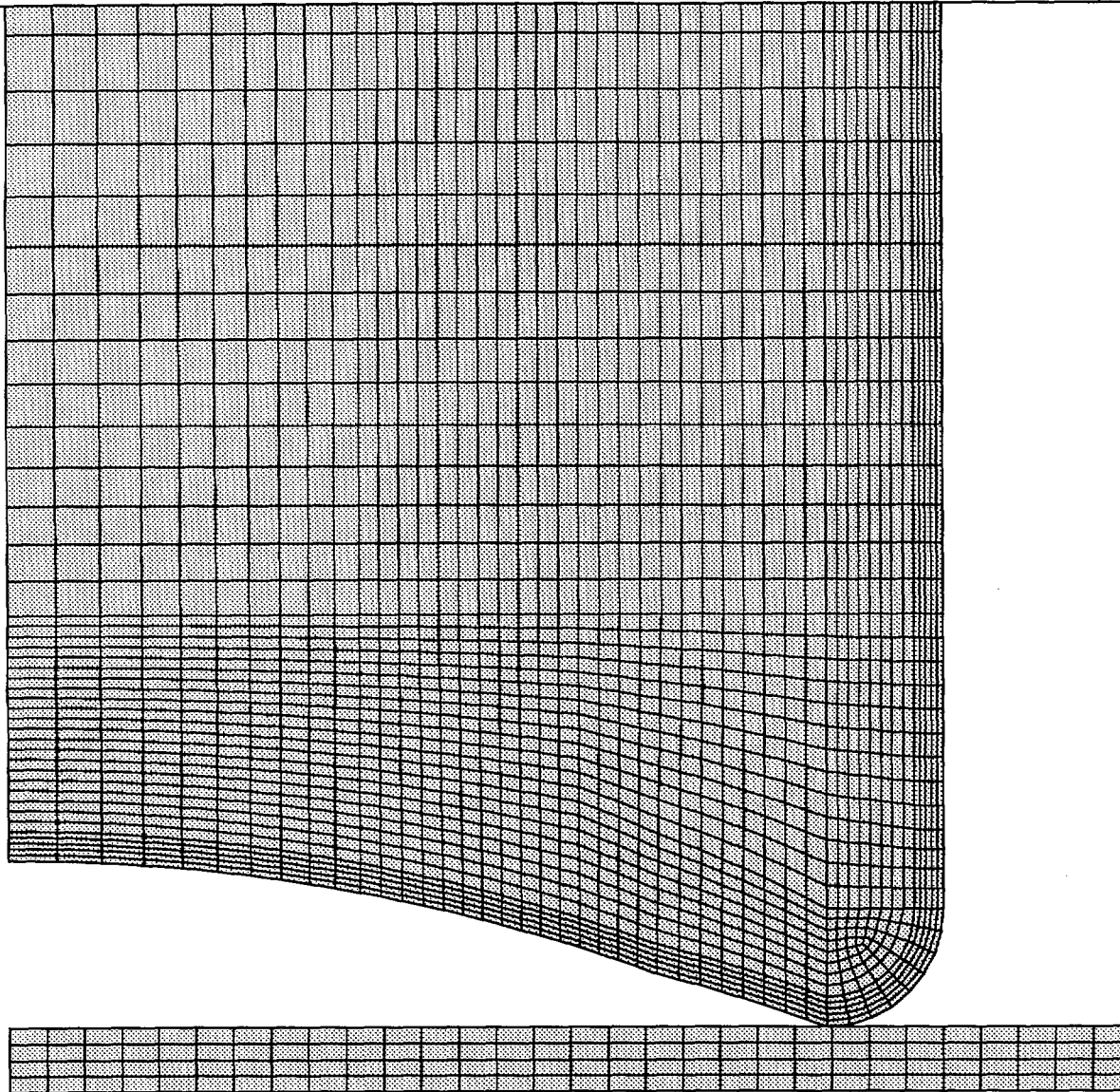
1



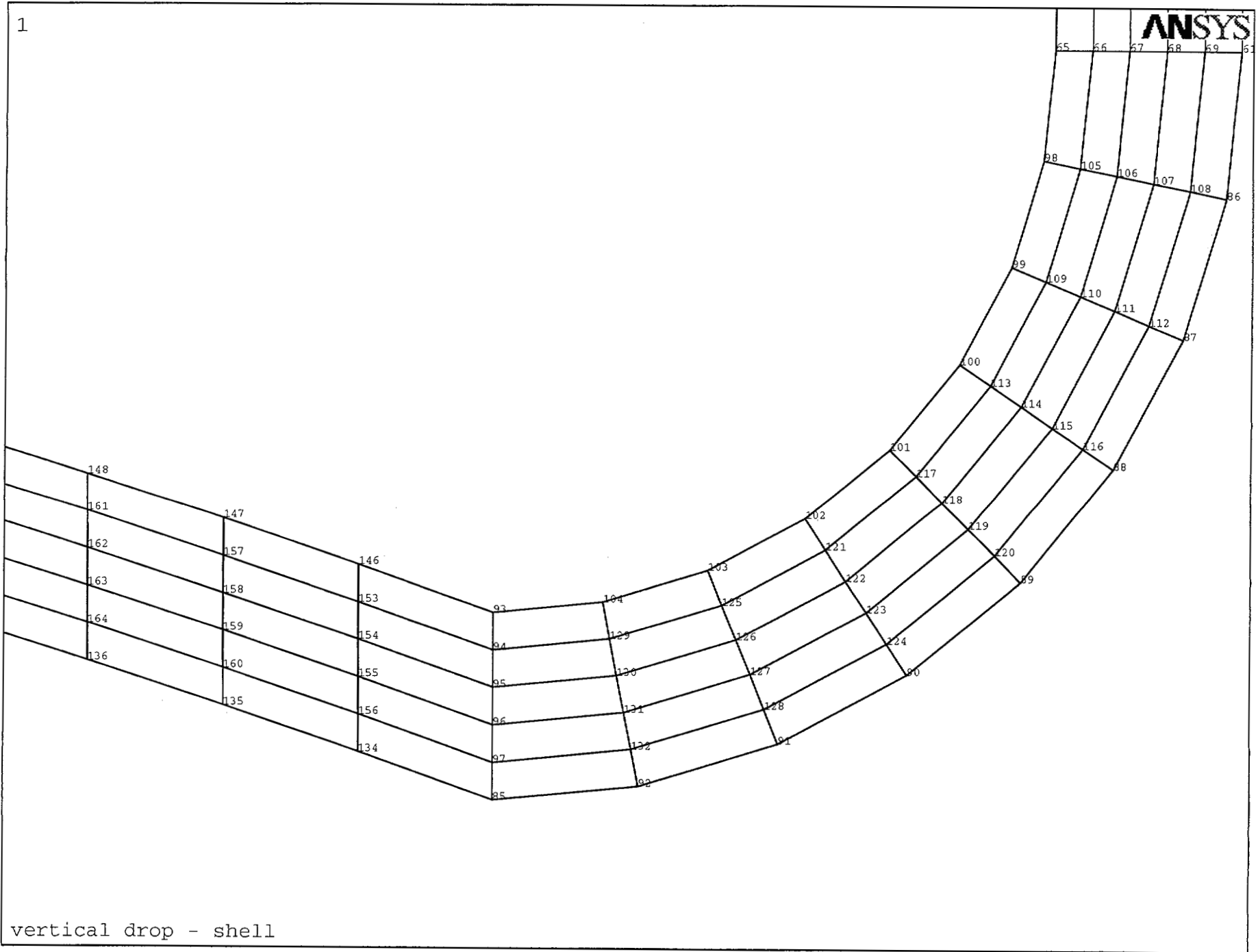
vertical drop

ANSYS

1



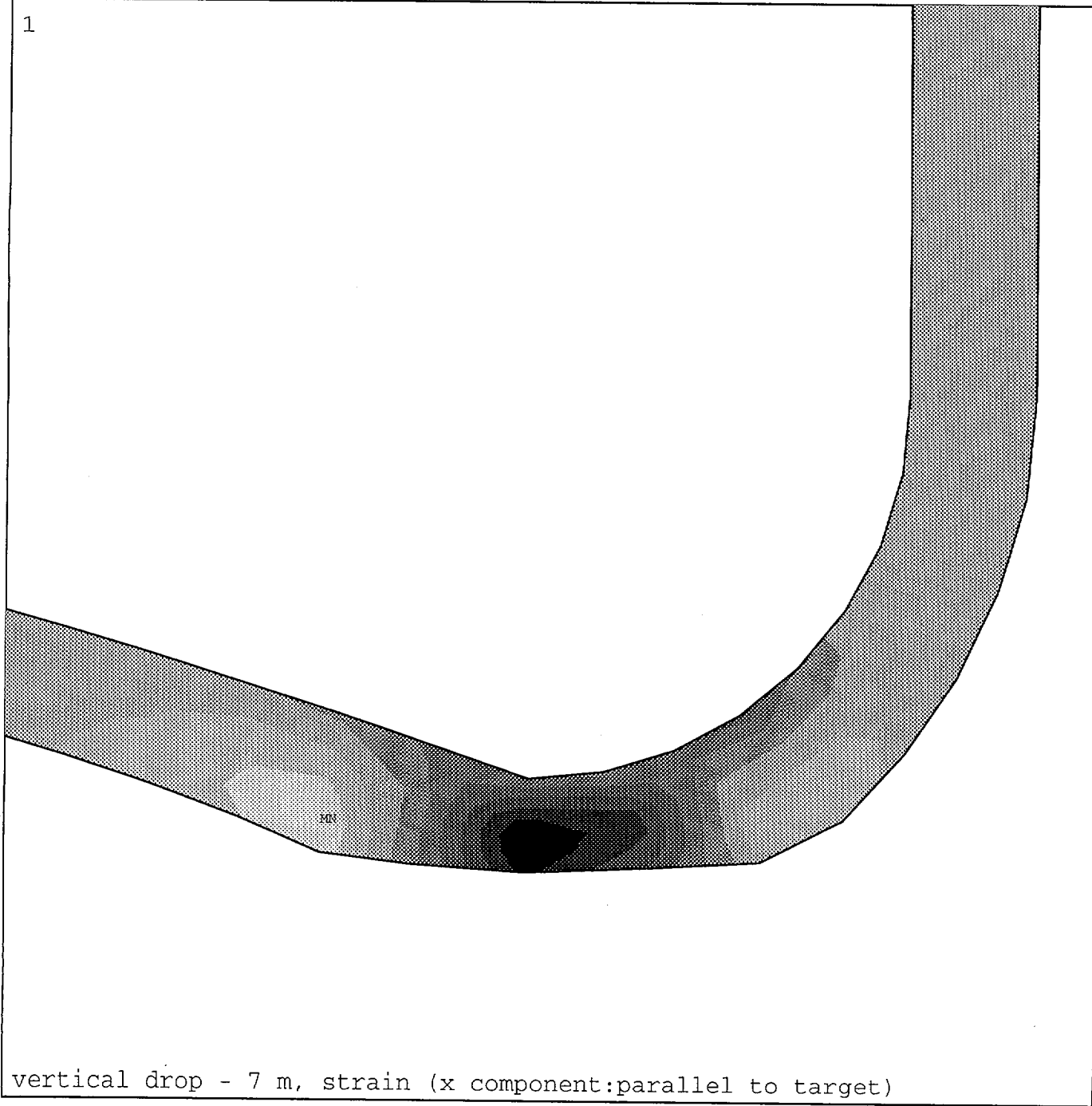
vertical drop



1











ANSYS 5.4
JUL 22 1999
13:33:40
PLOT NO. 1
NODAL SOLUTION
STEP=2
SUB =96
TIME=.001878
EPTOX (AVG)
RSYS=0
DMX =.003592
SMN =-.113763
SMX =.351619

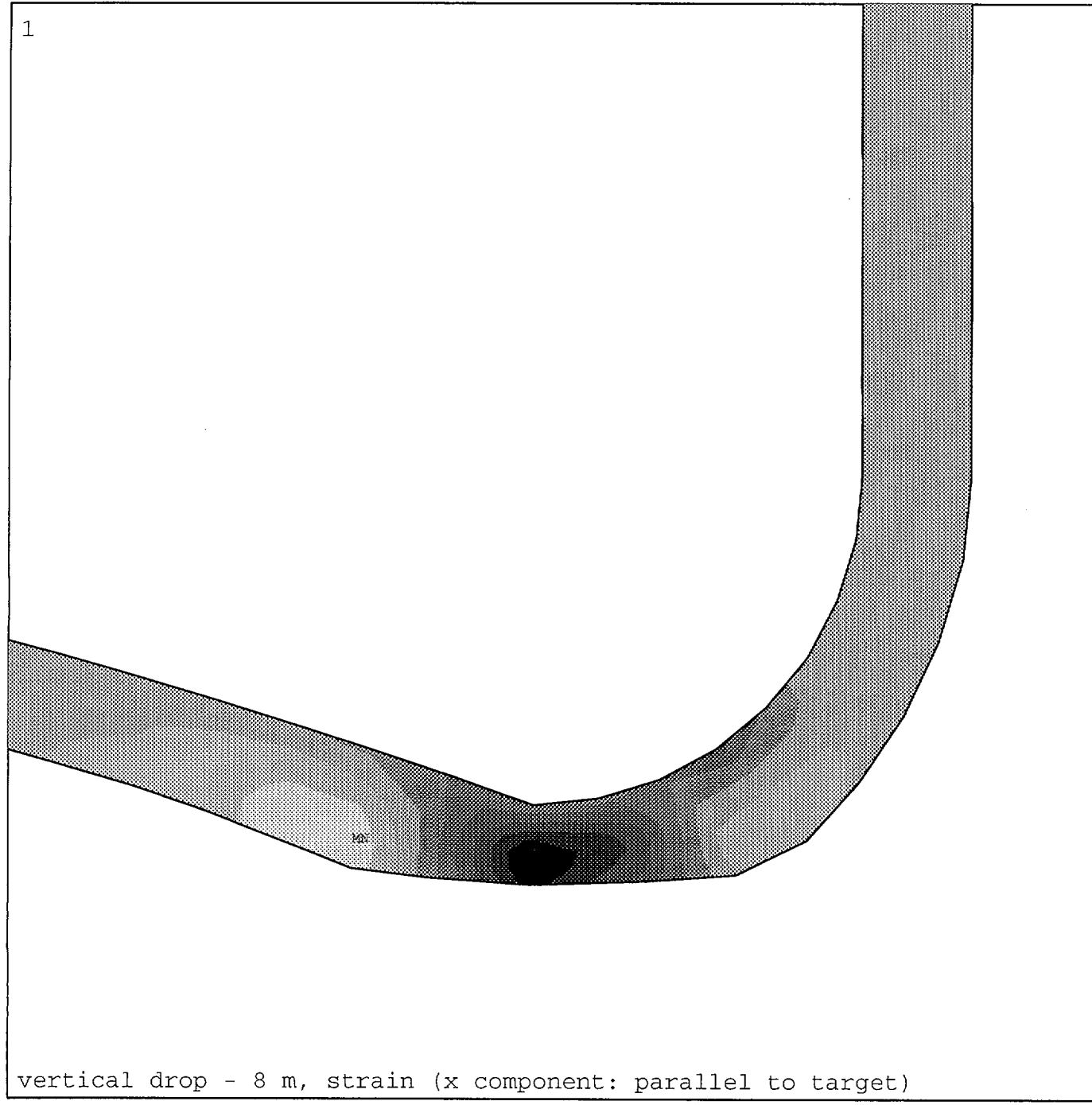
	-.113763
	-.062054
	-.010345
	.041364
	.093073
	.144783
	.196492
	.248201
	.29991
	.351619



1

ANSYS 5.4
JUL 22 1999
12:42:21
PLOT NO. 1
NODAL SOLUTION
STEP=2
SUB =80
TIME=.001834
EPTOX (AVG)
RSYS=0
DMX =.003861
SMN =-.109388
SMX =.369788

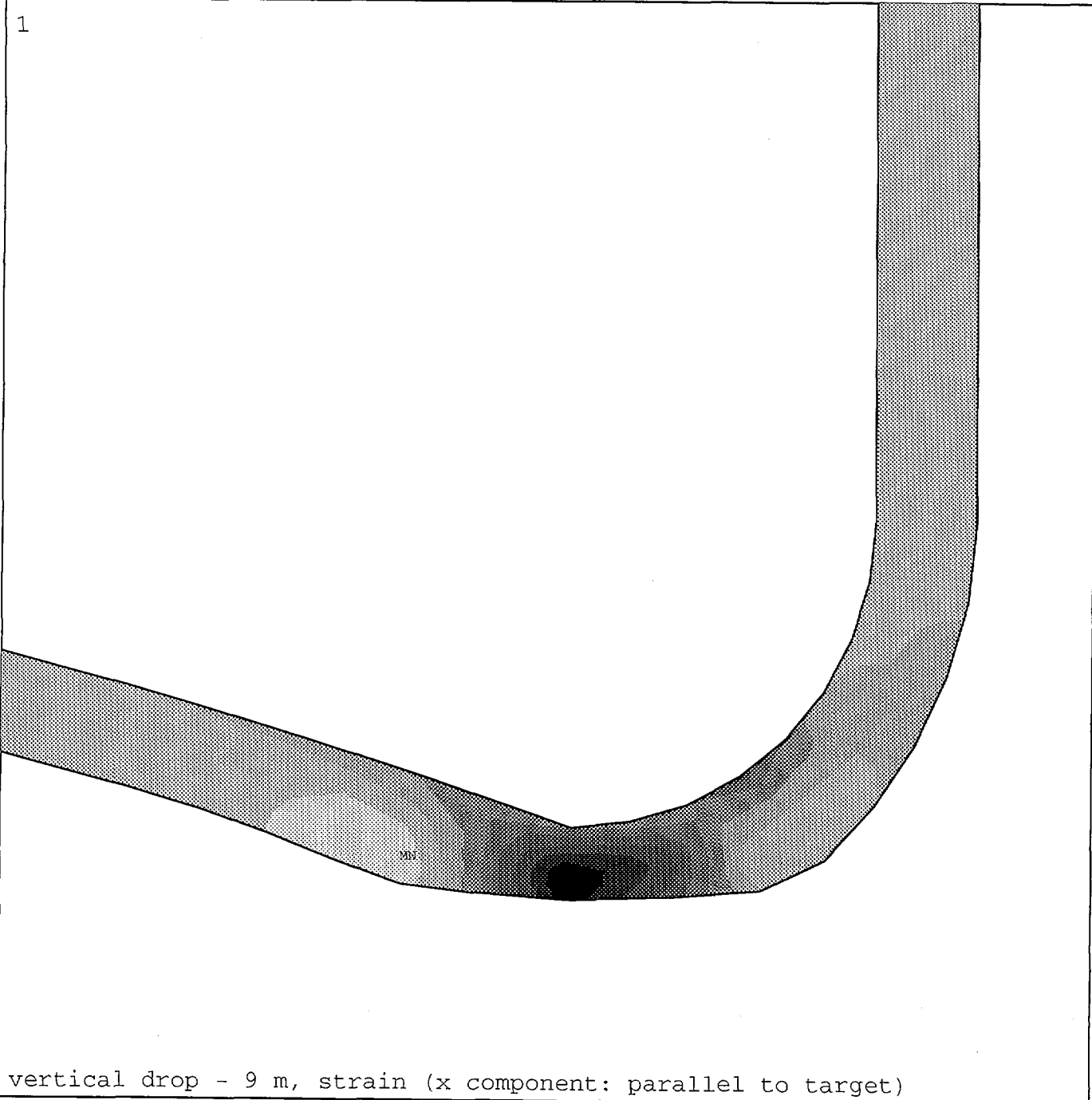
	-.109388
	-.056146
	-.002905
	.050337
	.103579
	.156821
	.210063
	.263304
	.316546
	.369788



vertical drop - 8 m, strain (x component: parallel to target)

ANSYS 5.4
JUL 22 1999
12:47:14
PLOT NO. 1
NODAL SOLUTION
STEP=2
SUB =94
TIME=.002268
EPTOX (AVG)
RSYS=0
DMX =.004473
SMN =-.102711
SMX =.39299

	-.102711
	-.047633
	.007445
	.062523
	.1176
	.172678
	.227756
	.282834
	.337912
	.39299

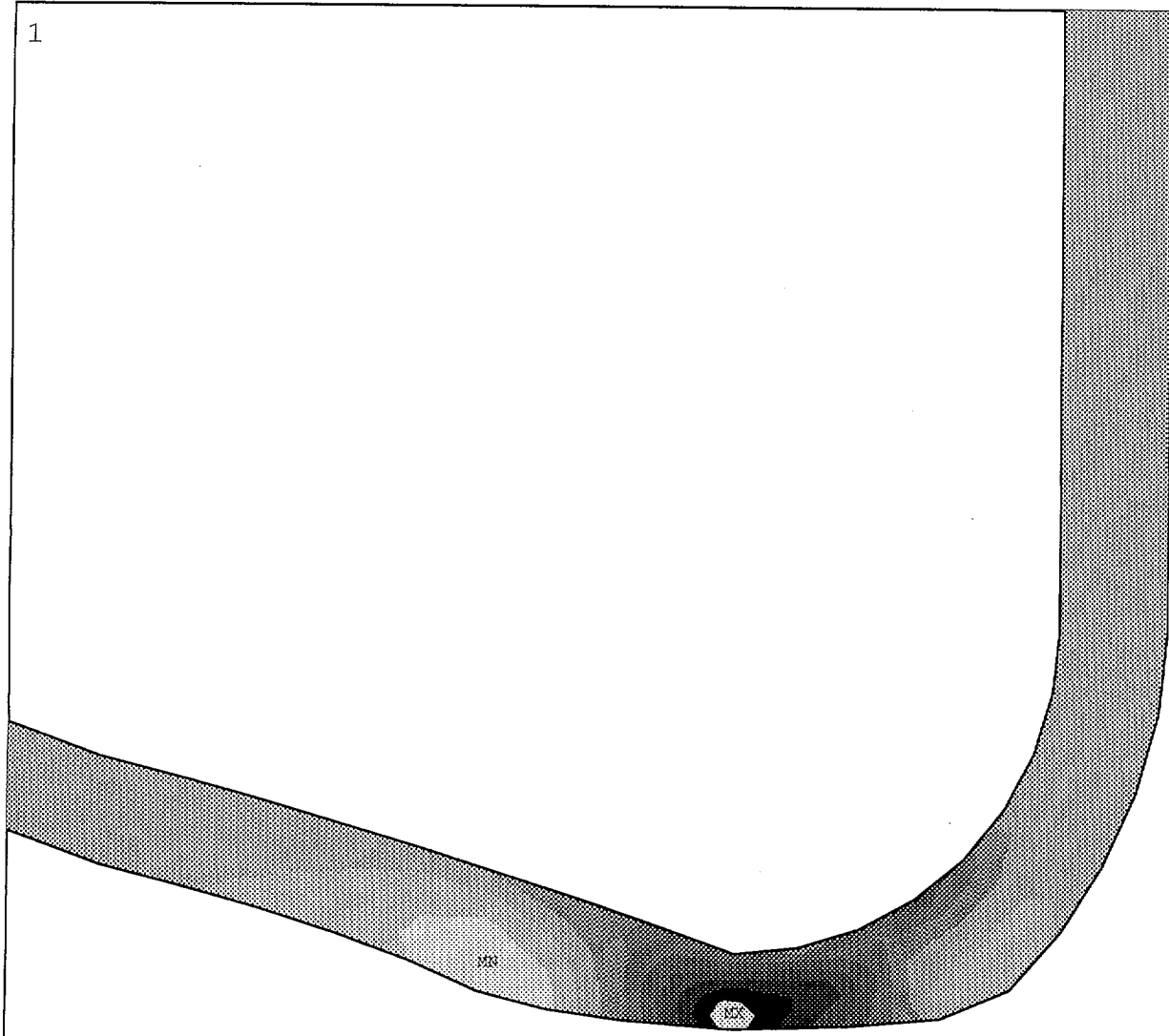


vertical drop - 9 m, strain (x component: parallel to target)

1

ANSYS 5.4
 JUL 22 1999
 13:22:00
 PLOT NO. 1
 NODAL SOLUTION
 STEP=2
 SUB =87
 TIME=.002181
 EPTOX (AVG)
 RSYS=0
 DMX =.004376
 SMN =-.119112
 SMX =.447263

[Lightest Grey]	-.119112
[Light Grey]	-.061433
[Medium-Light Grey]	-.003754
[Medium Grey]	.053925
[Medium-Dark Grey]	.111604
[Dark Grey]	.169284
[Very Dark Grey]	.226963
[Darkest Grey]	.284642
[Black]	.342321
[Black]	.4

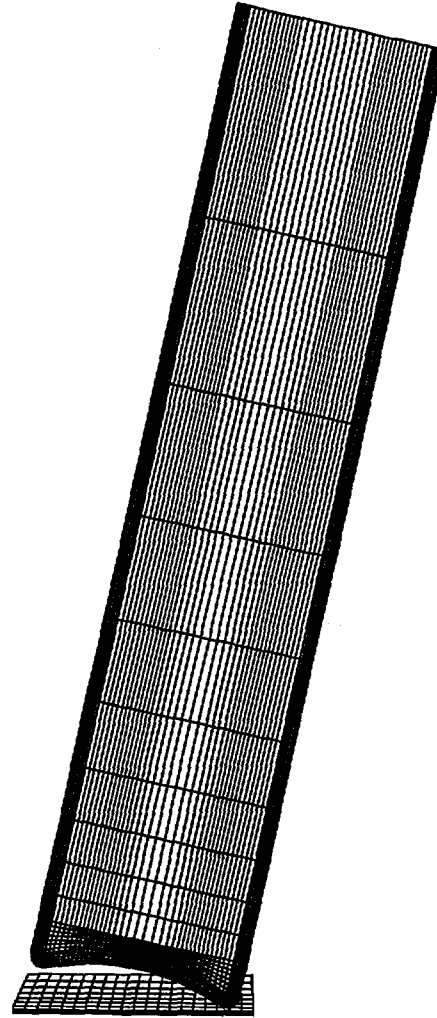


↑
 Note: Material with strain > 0.4 is shown in light grey.

vertical drop - 11.58 m, strain (x component:parallel to target)



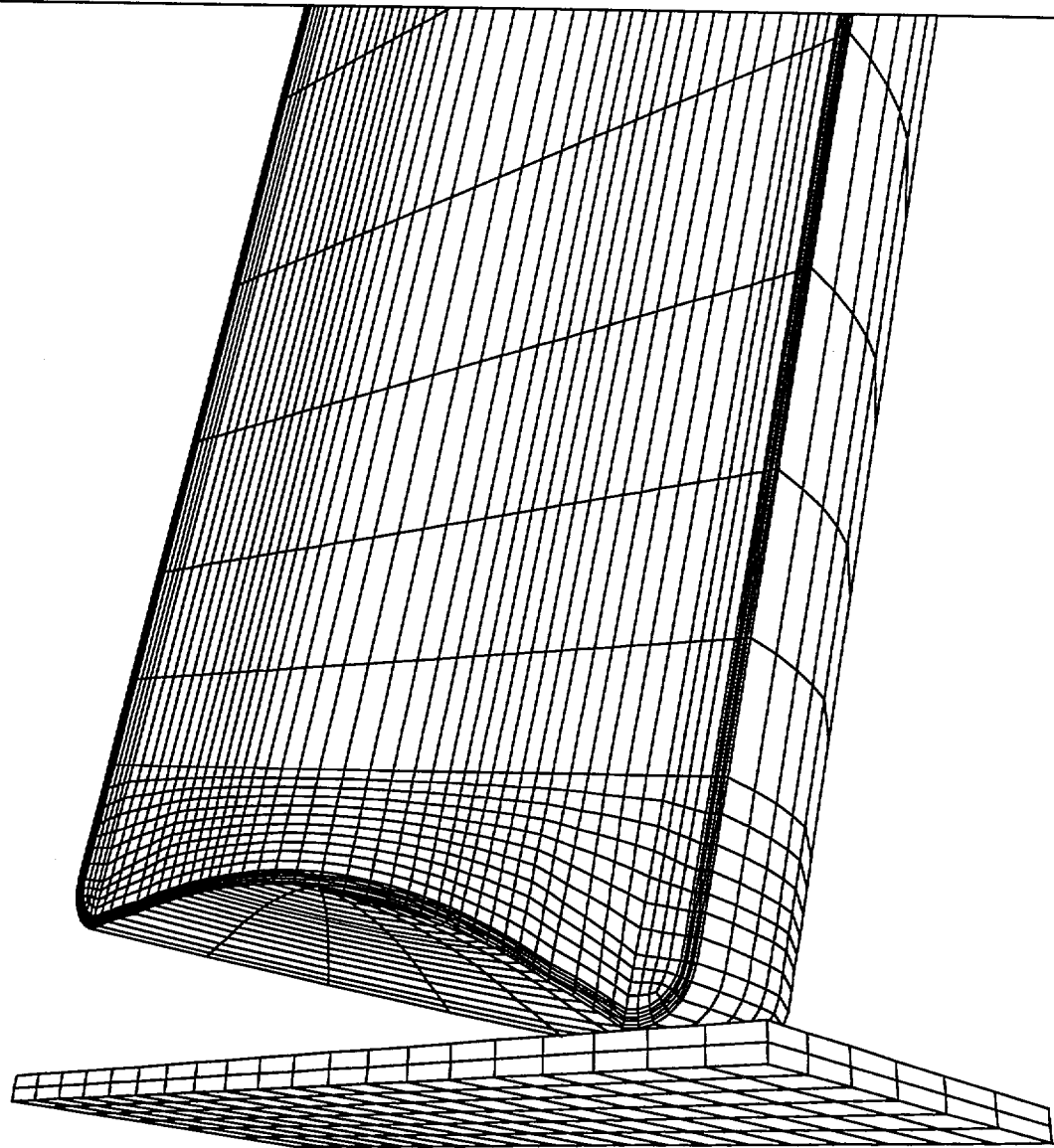
1



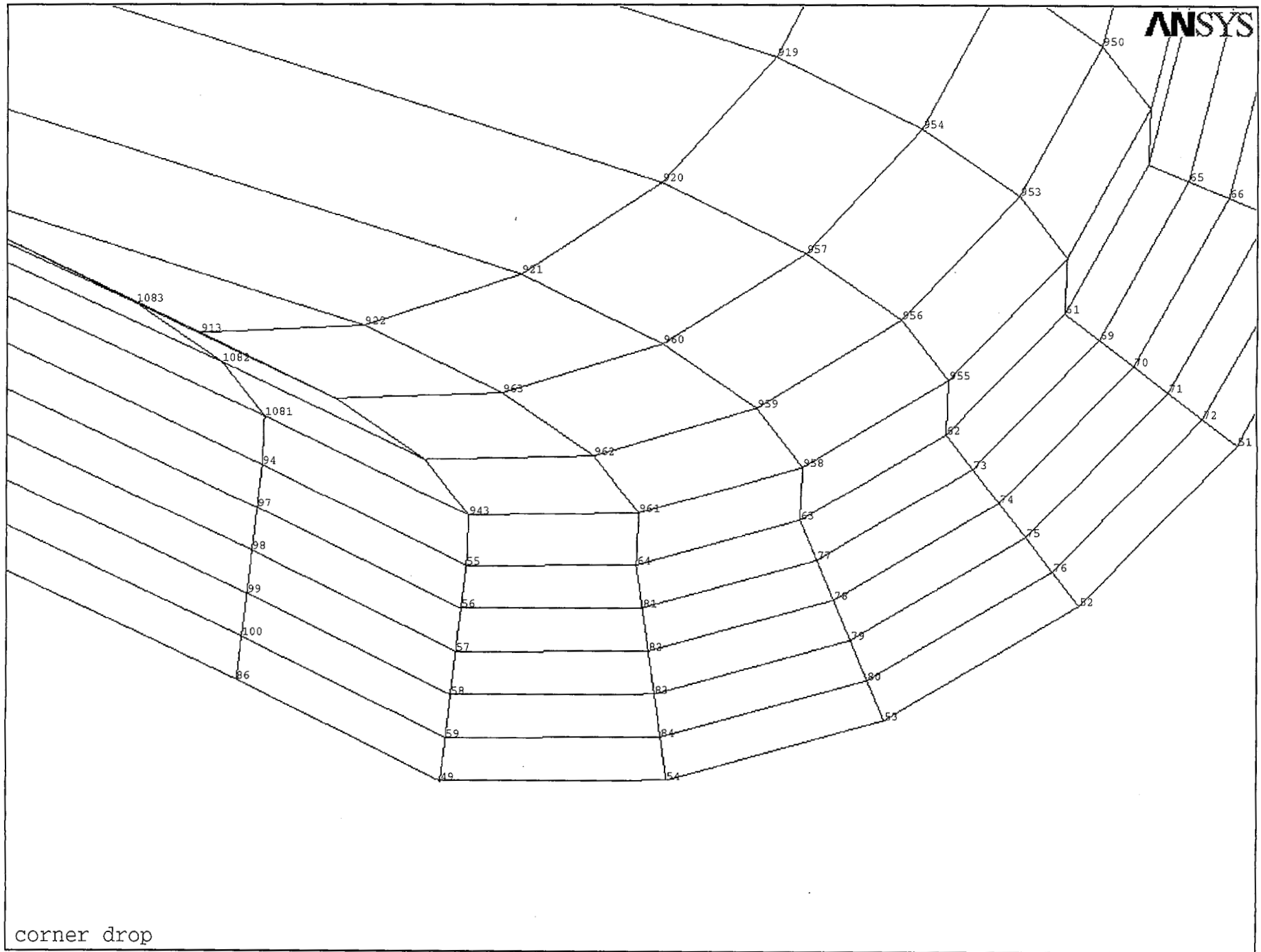
corner drop



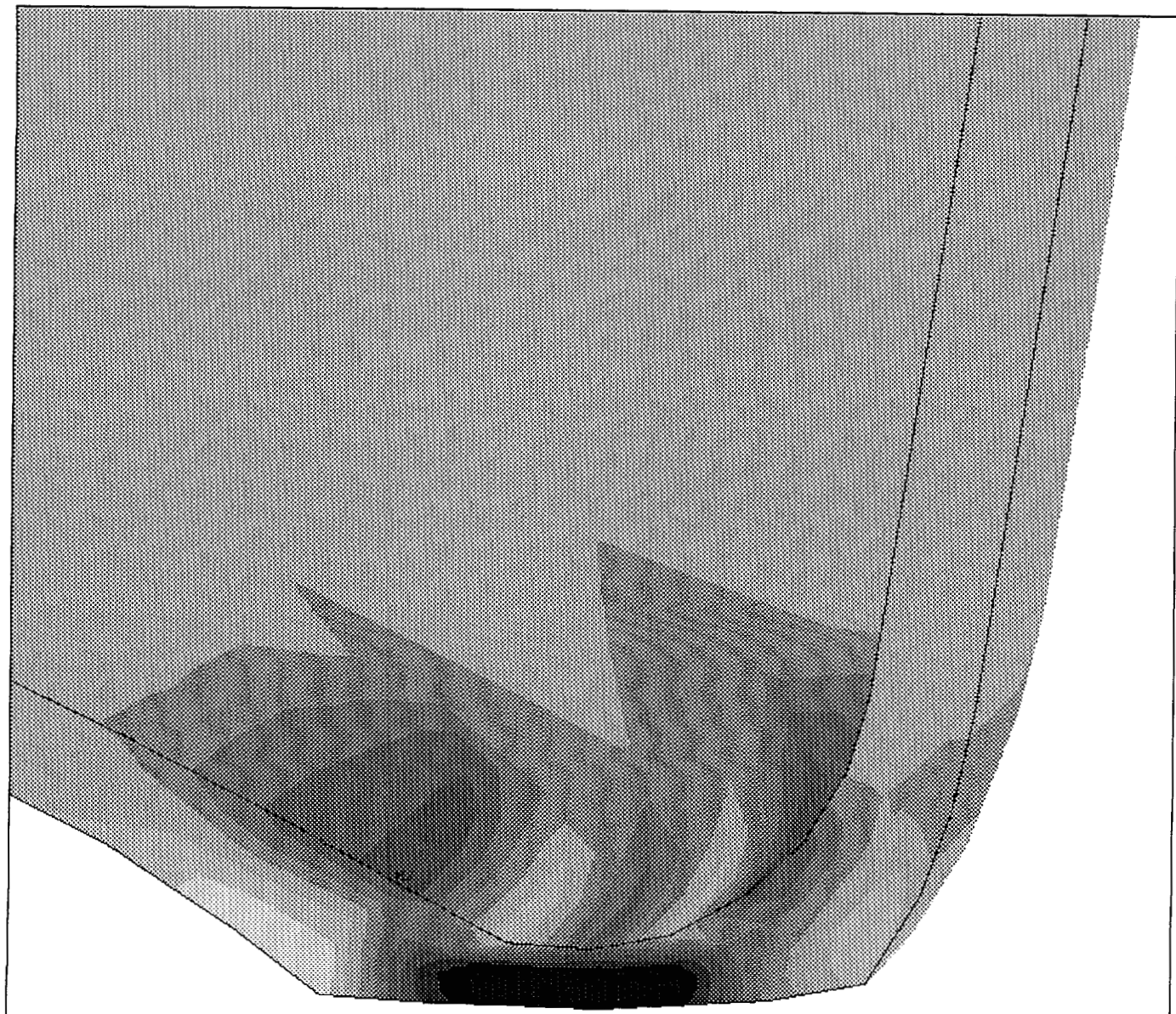
1



corner drop

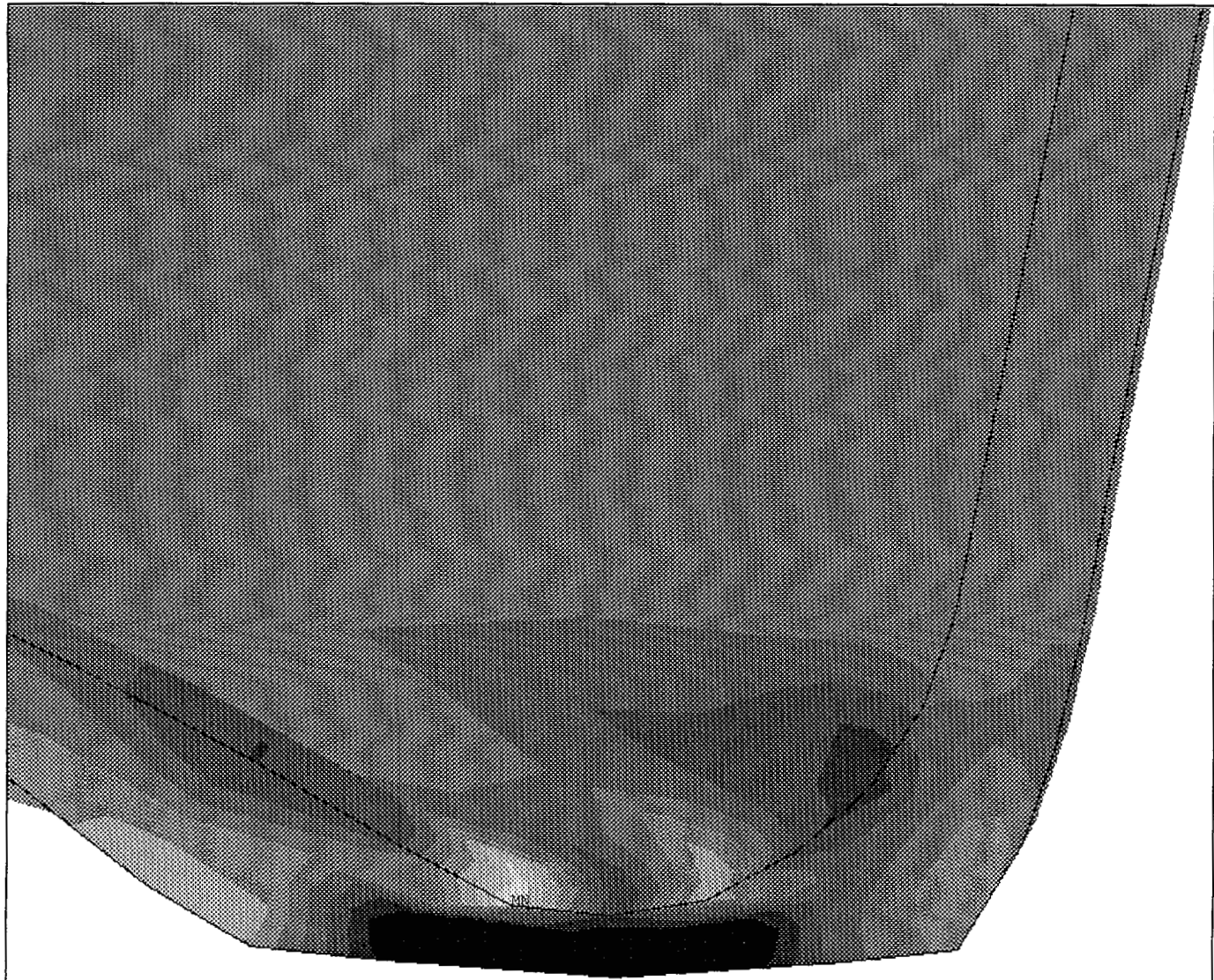


ANSYS 5.4
AUG 2 1999
12:50:39
PLOT NO. 1
NODAL SOLUTION
STEP=3
SUB =8
TIME=.0037
EPTOX (AVG)
RSYS=11
DMX =.0104
SMN =-.132335
SMX =.706443
-.132335
-.073187
-.014038
.04511
.104258
.163407
.222555
.281703
.340852
.4



↑
Note: Material with strain > 0.4 is shown in dark grey.

corner drop - 2 m, strain (x component: parallel to target)



ANSYS 5.4
AUG 2 1999
13:46:24
PLOT NO. 1
NODAL SOLUTION
STEP=2
SUB =79
TIME=.003783
EPTOX (AVG)
RSYS=11
DMX =.014632
SMN =-.343396
SMX =.888002

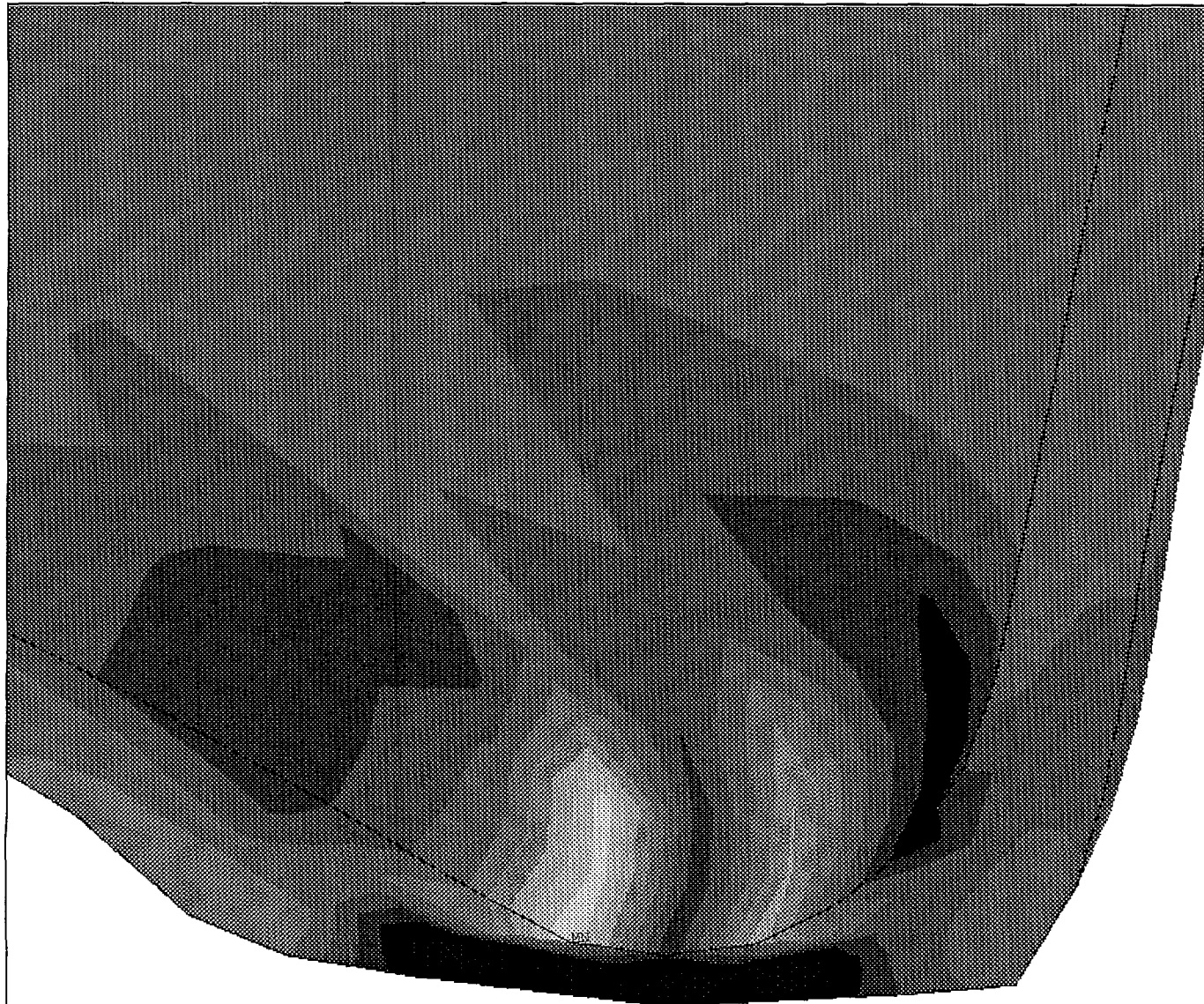
Lightest grey	-.343396
Light grey	-.260796
Medium-light grey	-.178197
Medium grey	-.095597
Medium-dark grey	-.012998
Dark grey	.069602
Very dark grey	.152201
Blackish grey	.234801
Dark grey	.3174
Darkest grey	.4

↑

Note: Material with strain > 0.4 is shown in dark grey.

corner drop - 4 m, strain (x component: parallel to target)











ANSYS 5.4
AUG 2 1999
13:59:59
PLOT NO. 1
NODAL SOLUTION
STEP=2
SUB =87
TIME=.003537
EPTOX (AVG)
RSYS=11
DMX =.017772
SMN =-.653039
SMX =1.01
-.653039
-.536035
-.41903
-.302026
-.185022
-.068017
.048987
.165991
.282996
.4

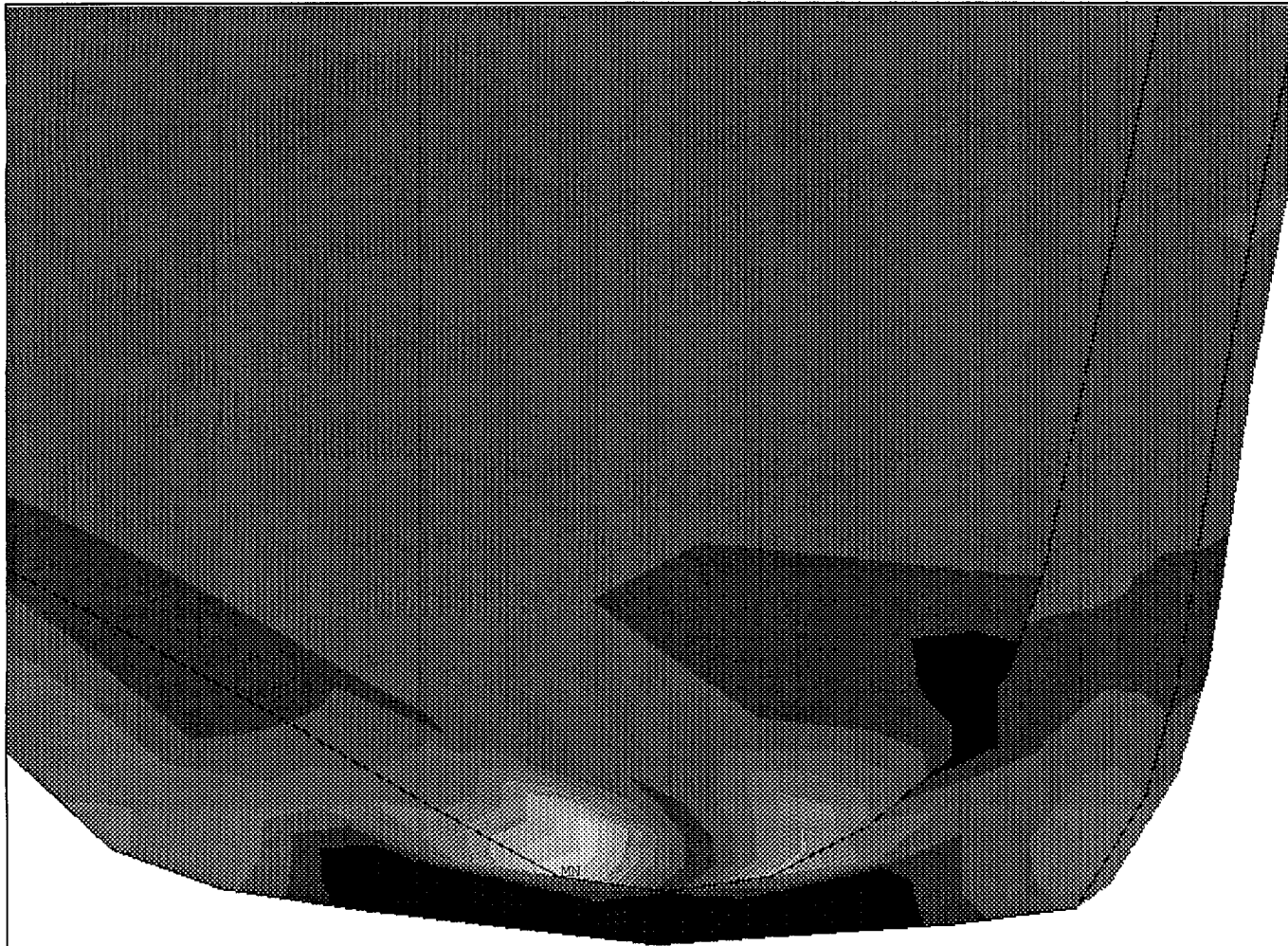


↑
Note: Material with strain > 0.4 is shown in dark grey.

corner drop - 7 m, strain (x component: parallel tp target)

ANSYS 5.4
AUG 2 1999
14:10:19
PLOT NO. 1
NODAL SOLUTION
STEP=3
SUB =16
TIME=.003396
EPTOX (AVG)
RSYS=11
DMX =.019838
SMN =-.823787
SMX =1.074

	-.823787
	-.687811
	-.551834
	-.415858
	-.279882
	-.143905
	-.007929
	.128047
	.264024
	.4

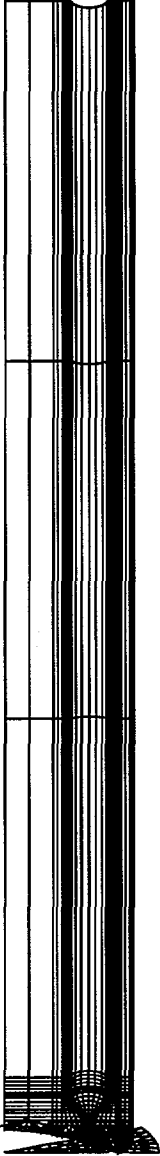


Note: Material with strain > 0.4 is shown in dark grey.

corner drop - 9.14 m, strain (x component: parallel to target)

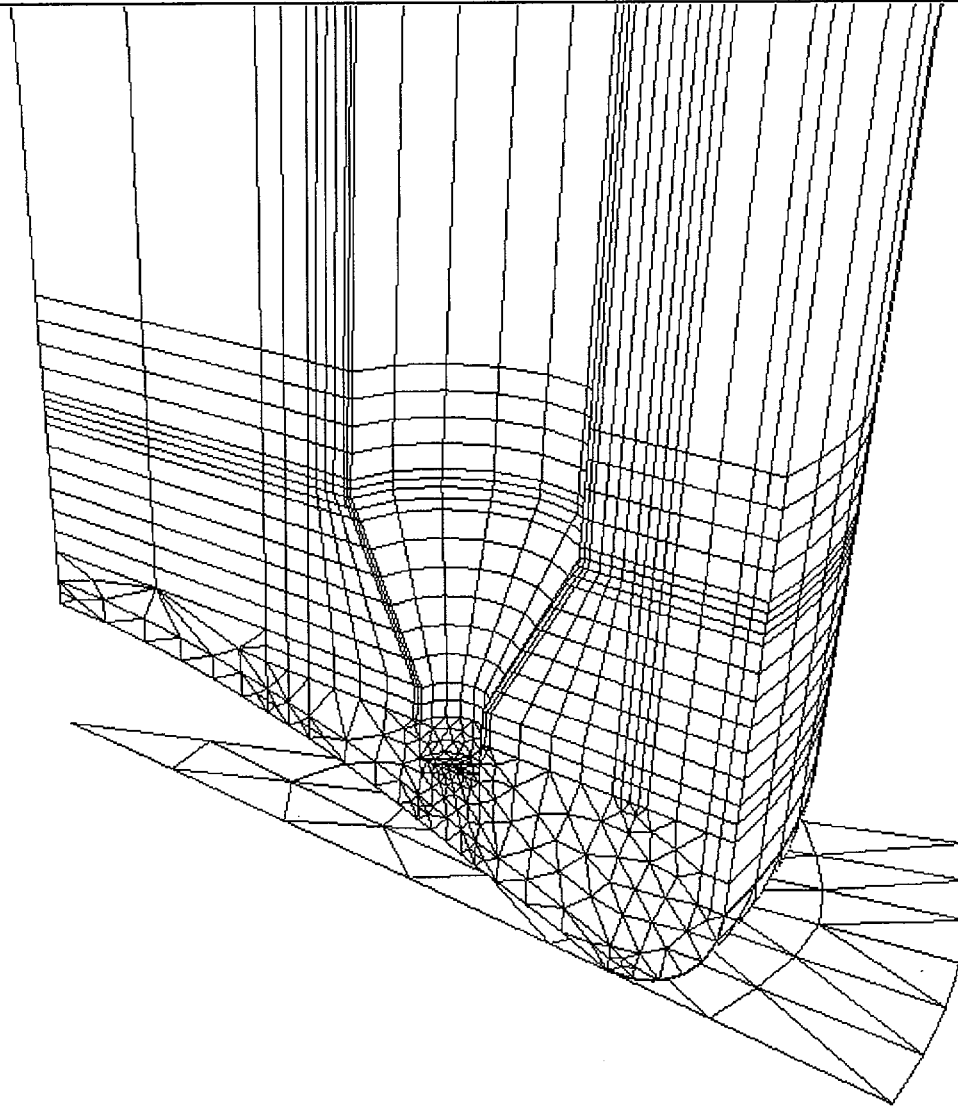


1



can-in-canister vertical drop

ANSYS



can-in-canister vertical drop